



Overview of results from ALICE

- Particle production and collective flow
- Correlations and Fluctuations
- Summary and Outlook

UJ 22.03.2021 (virtual ☺)

Jacek Otwinowski (IFJ PAN, Krakow)
On behalf of the ALICE Collaboration

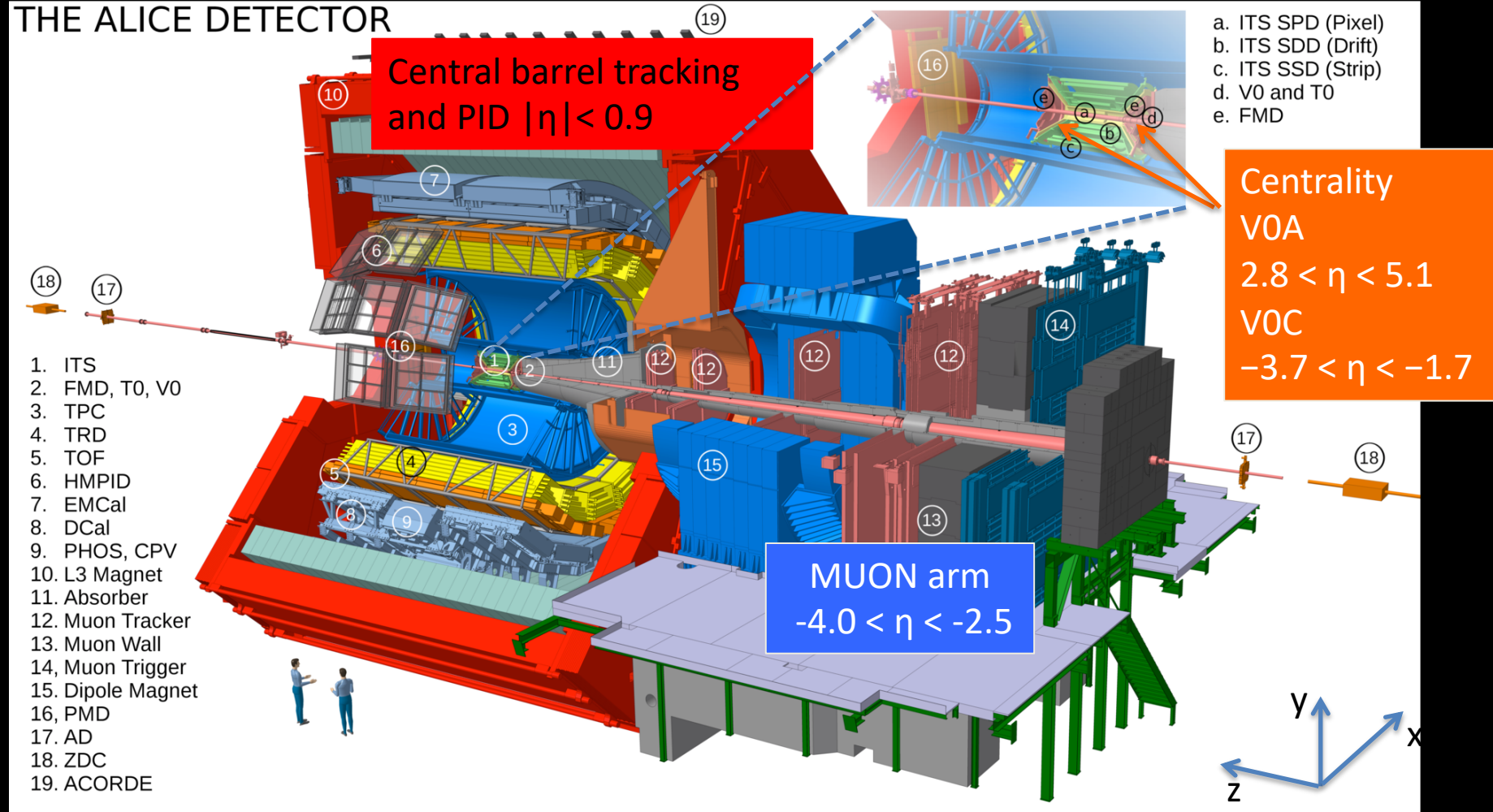


A Large Ion Collider Experiment



- Excellent particle identification capabilities over a wide p_T range 0.1-20 GeV/c
- Good momentum resolution $\sim 1\text{-}5\%$ for $p_T = 0.1\text{-}50$ GeV/c

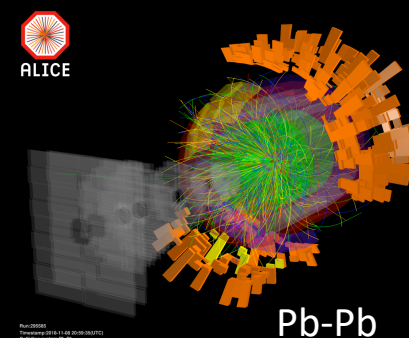
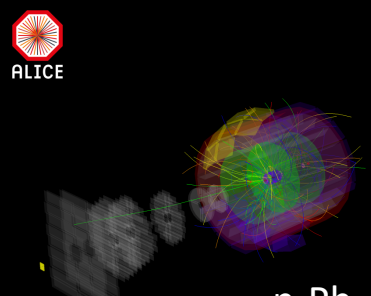
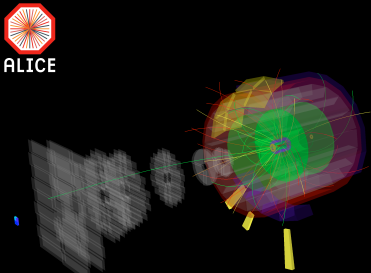
THE ALICE DETECTOR



ALICE at work since 2009



System	Year	\sqrt{s}_{NN} (TeV)	L_{int}
Pb-Pb	2010-2011	2.76	$\sim 75 \mu\text{b}^{-1}$
	2015	5.02	$\sim 250 \mu\text{b}^{-1}$
	2018	5.02	$\sim 0.9 \text{ nb}^{-1}$
Xe-Xe	2017	5.44	$\sim 0.3 \mu\text{b}^{-1}$
p-Pb	2013	5.02	$\sim 15 \text{ nb}^{-1}$
	2016	5.02, 8.16	$\sim 3 \text{ nb}^{-1}, \sim 25 \text{ nb}^{-1}$
pp	2009-2013	0.9, 2.76, 7, 8	$\sim 200 \mu\text{b}^{-1}, \sim 100 \mu\text{b}^{-1},$ $\sim 1.5 \text{ pb}^{-1}, \sim 2.5 \text{ pb}^{-1}$
	2015-2018	5.02, 13	$\sim 1.3 \text{ pb}^{-1}, \sim 59 \text{ pb}^{-1}$

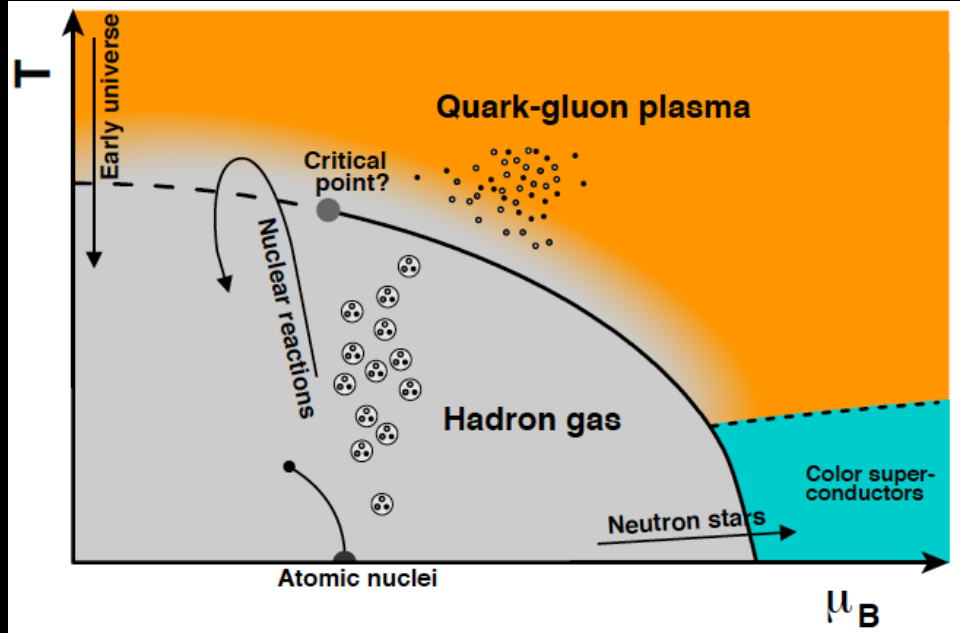


- Energy and system dependence studies of particle production are possible
- Large statistics of pp, p-Pb and Pb-Pb collisions at the same \sqrt{s}_{NN}
→ Precise comparison studies

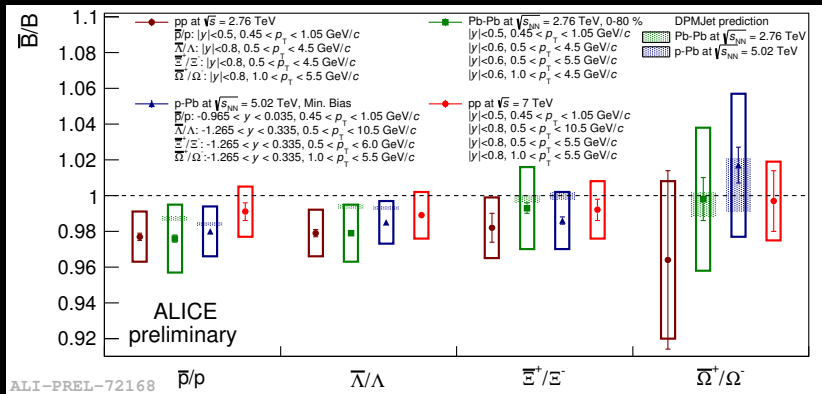
Study of the quark-gluon plasma

ALICE case

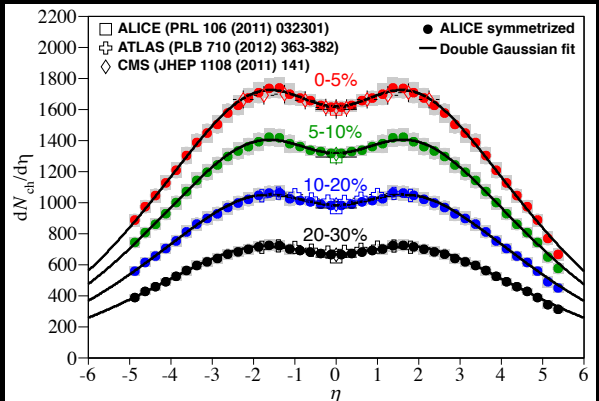
ALICE probes nuclear matter at $\mu_B \sim 0$ and high temperature



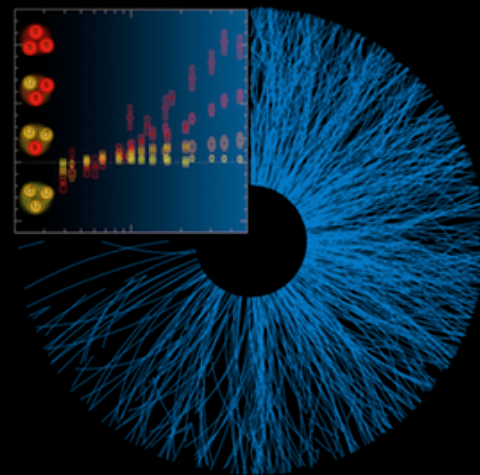
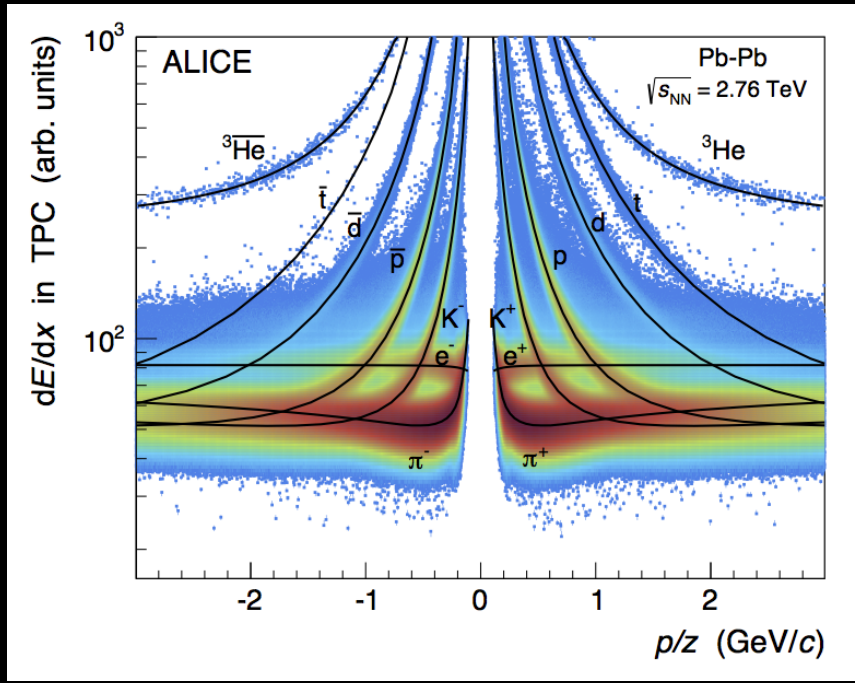
Lattice QCD: Hadron gas to quark-gluon plasma
 $(\mu_B = 0, T_C = 156.5 \pm 1.5 \text{ MeV},$
 $\epsilon_C = (0.42 \pm 0.06) \text{ GeV/fm}^3$, smooth crossover)
A. Bazavov et al. Phys. Lett. B 795 (2019) 15



Phys. Lett. B 726 (2013) 610-622



Central collisions:
 $\epsilon \sim 14 \text{ GeV/fm}^3 >> \epsilon_c$



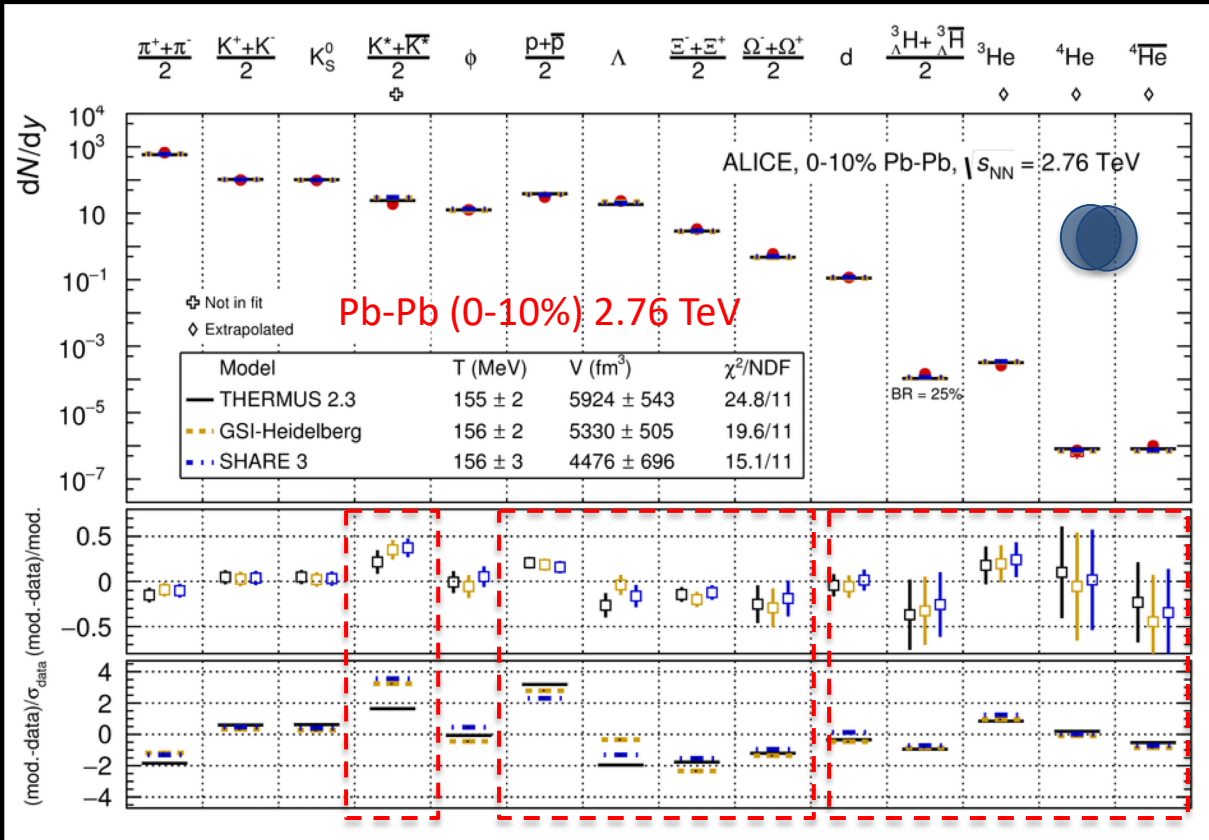
PARTICLE PRODUCTION

Hadron yields vs thermal models in Pb-Pb

at $\sqrt{s}_{\text{NN}} = 2.76 \text{ TeV}$



Nucl. Phys. A 971 (2018) 1



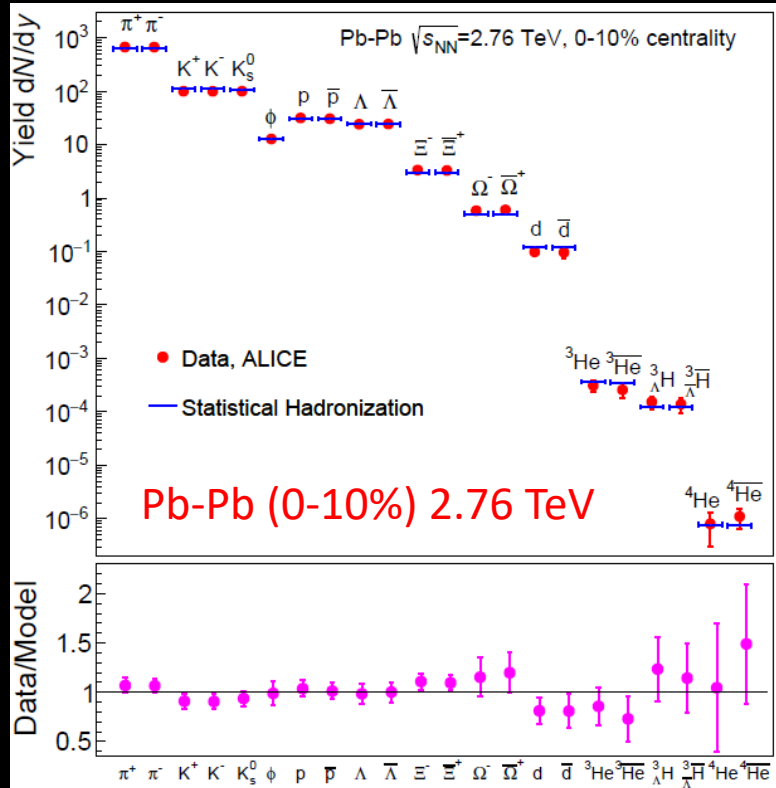
- Production of (most) hadrons well described at freezeout temperature $T_{\text{ch}} \sim 156 \text{ MeV}$
- K^*0 resonance (not included in the fit): production overestimated by thermal models
- Tension for protons and multi-strange baryons
- Light nuclei production described by thermal models (binding energy $\ll T_{\text{ch}}$)?

THERMUS: Wheaton et al., Comput. Phys. Commun. 180 (2009) 84

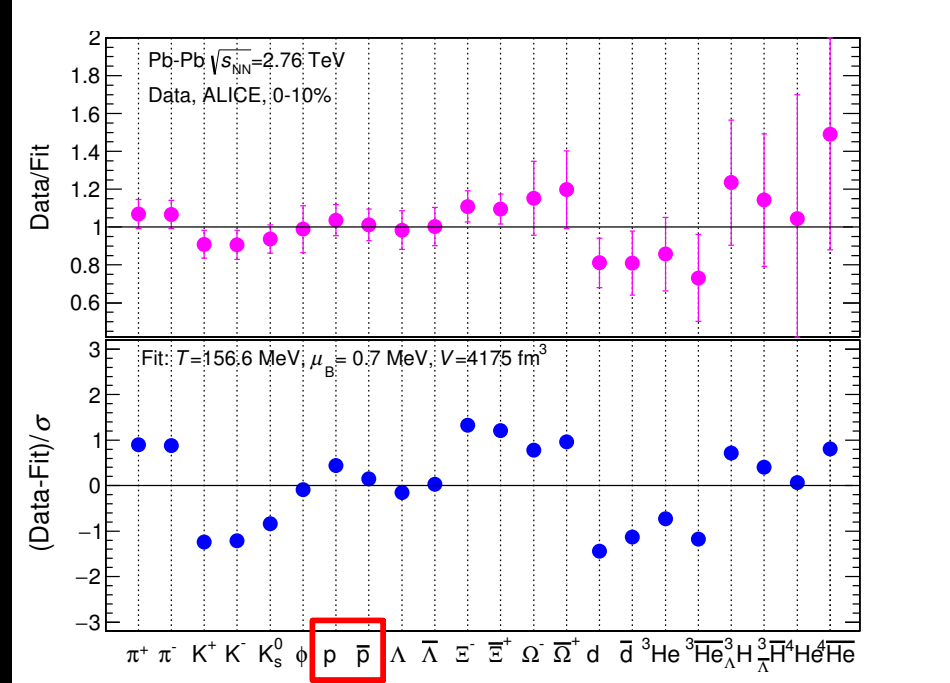
GSI-Heidelberg: Andronic et al., Phys. Lett. B 673 142

SHARE: Petran et al., Comp. Phys. Commun. 195 (2014) 2056

Hadron yields vs improved thermal model in Pb-Pb at $\sqrt{s}_{\text{NN}} = 2.76 \text{ TeV}$

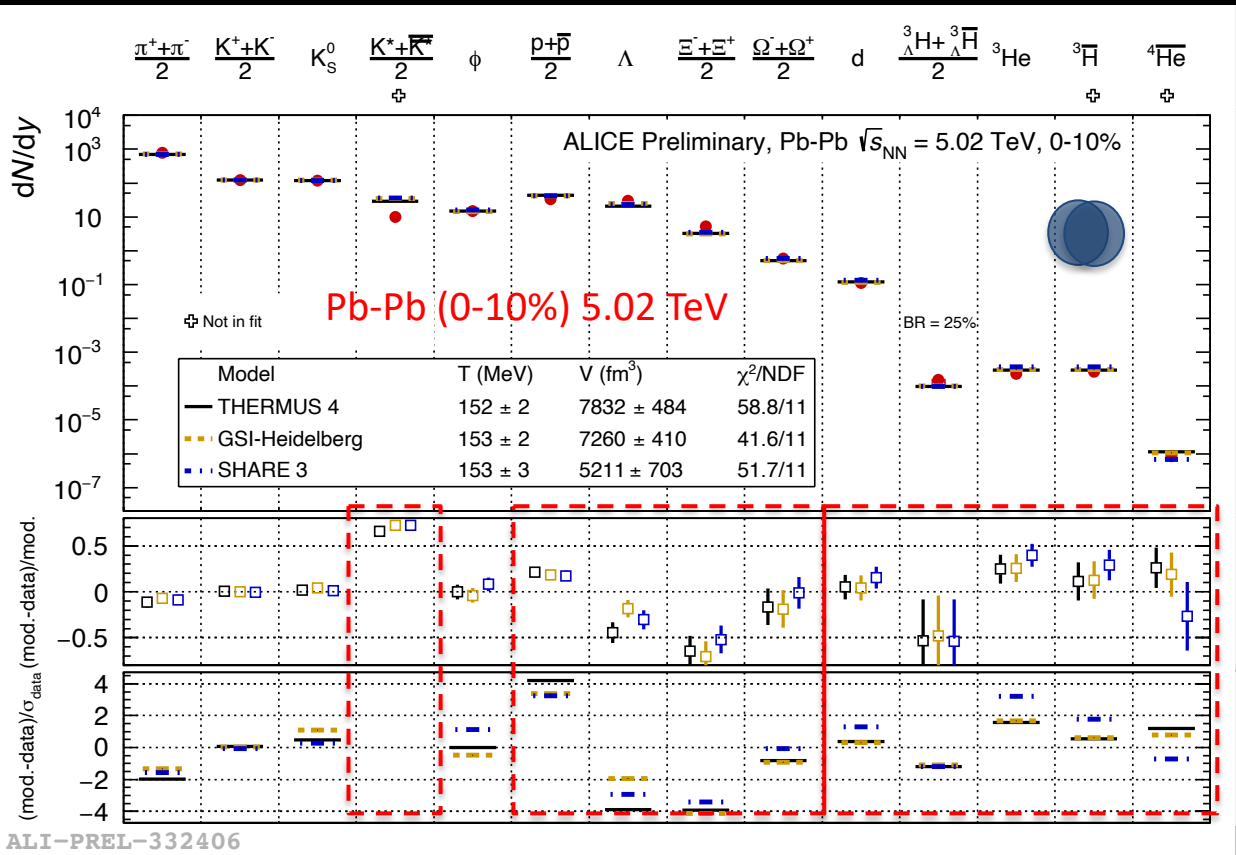


A. Andronic et al. Phys. Lett. B792 (2019) 304



- Resonant and non-resonant pion-nucleon and multi-pion-nucleon interactions included in the model (S-matrix approach)
- Production of hadrons well described at freezeout temperature $T_{\text{ch}} = 156.6 \pm 1.7 \text{ MeV}$
 → consistent with critical temperature T_c from the lattice QCD calculations

Particle yields vs thermal models in Pb-Pb at $\sqrt{s}_{\text{NN}} = 5.02 \text{ TeV}$



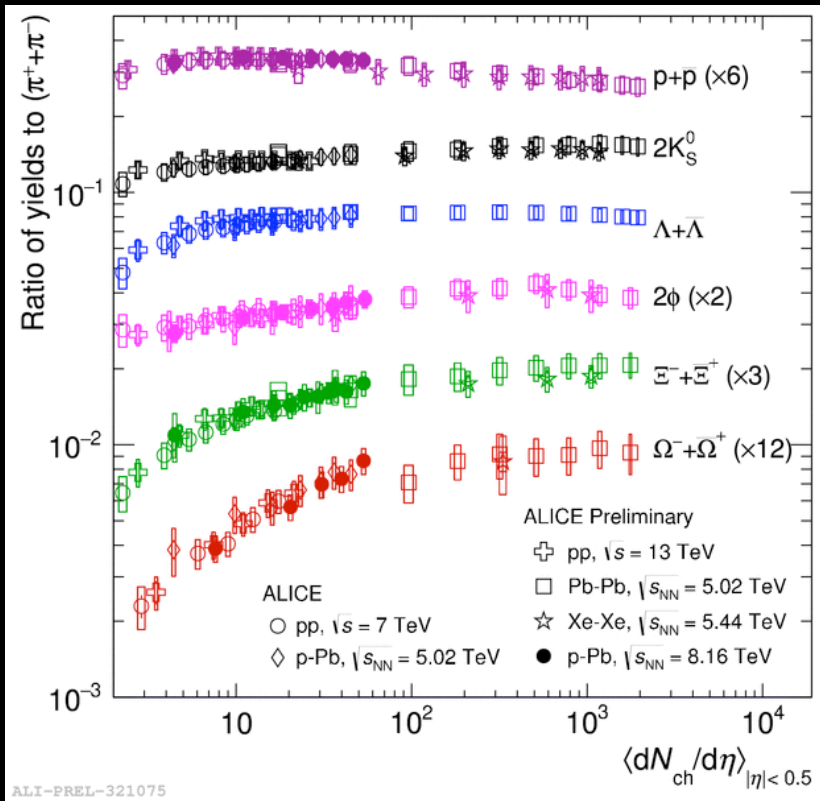
- Production of (most) hadrons well described at freeze-out temperature $T_{\text{ch}} \sim 153 \text{ MeV}$ (different than at 2.76 TeV)
- K^{*0} resonance (not included in the fit): production overestimated by thermal models
- Tension for protons and multi-strange baryons (new approach is currently studied)
- Light nuclei production described by thermal models (binding energy $\ll T_{\text{ch}}$)?

THERMUS: Wheaton et al., Comput. Phys. Commun. 180 (2009) 84

GSI-Heidelberg: Andronic et al., Phys. Lett. B 673 142

SHARE: Petran et al., Comp. Phys. Commun. 195 (2014) 2056

Relative particle production in pp, p-Pb, Pb-Pb and Xe-Xe



- Smooth evolution from pp to Pb-Pb
- No significant energy and system dependence is observed at similar multiplicity
- Relative strangeness production increases with multiplicity and strangeness content in small systems

→ Hadron production is driven by the characteristics of final state

pp 7 TeV: [Nature Physics 13 \(2017\) 535](#)

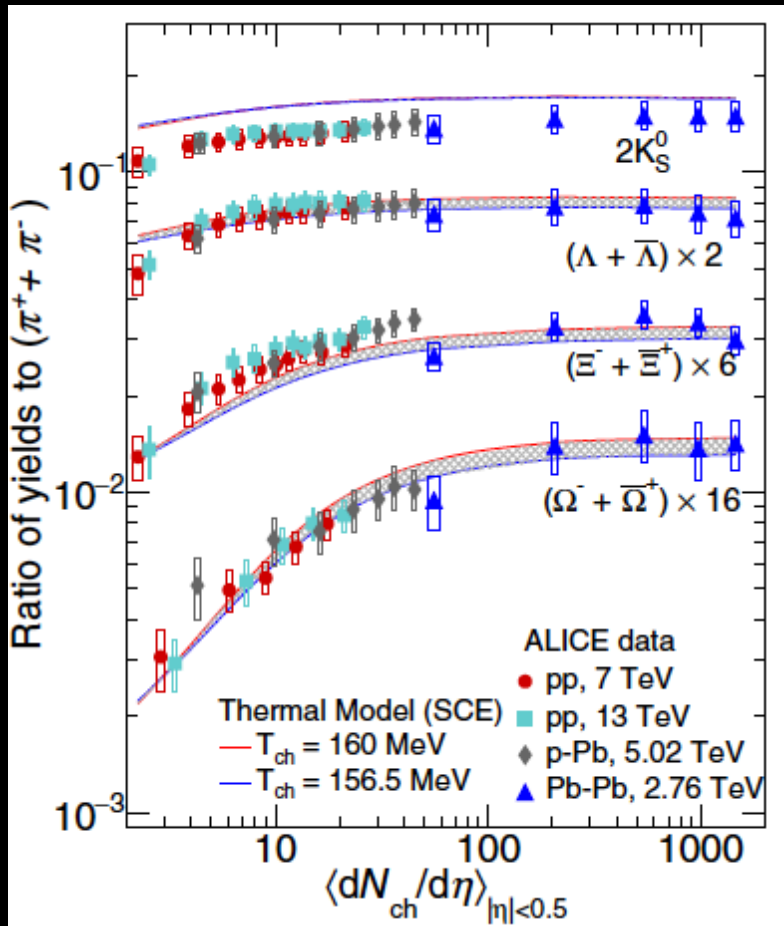
pp 7 and 13 TeV: [arXiv:2005.11120](#)

p-Pb 5.02 TeV: [Phys. Lett. B728 \(2014\) 25](#), [Phys. Lett. B758 \(2016\) 389](#)

Xe-Xe 5.44 TeV: [arXiv:2101.03100](#)

pp and Pb-Pb 5.02 TeV: [Phys. Rev. C 101, 044907 \(2020\)](#)

Relative particle production in pp, p-Pb, Pb-Pb and Xe-Xe



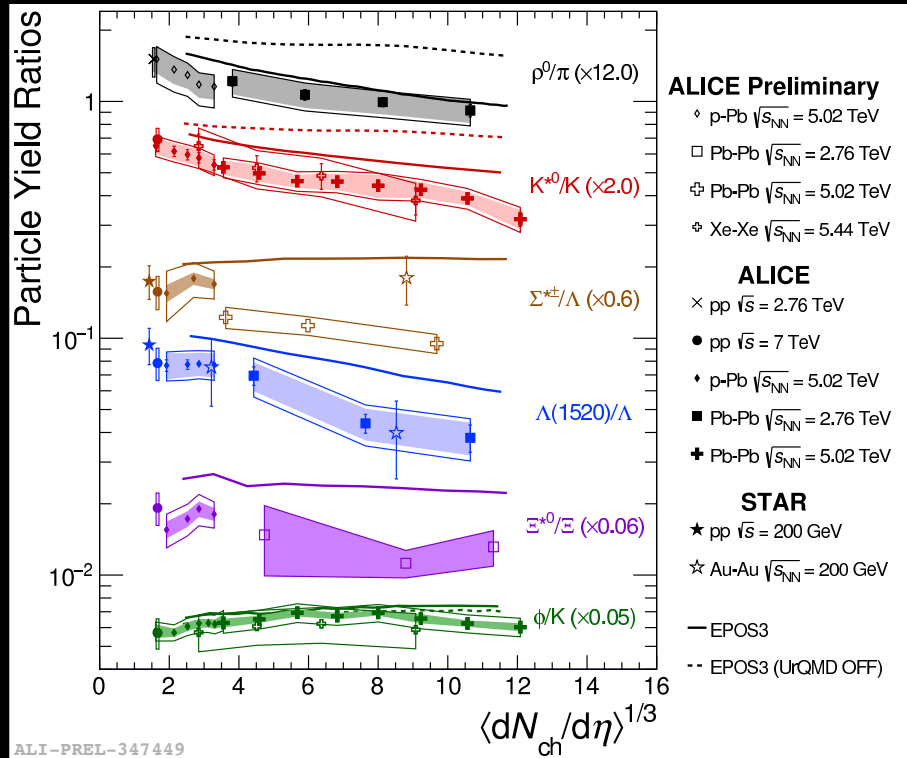
- Smooth evolution from pp to Pb-Pb
- No significant energy and system dependence is observed at similar multiplicity
- Relative strangeness production increases with multiplicity and strangeness content in small systems
- Thermal model (SCE) including interaction between hadrons (S-matrix approach) and exact strangeness conservation J. Cleymans et al. Phys. Rev. C103 014904 (2021)

pp 7 TeV and Pb-Pb 2.76 TeV: Nature Physics 13 (2017) 535
pp 7 and 13 TeV: arXiv:2005.11120

Relative resonance production in pp, p-Pb, Pb-Pb and Xe-Xe collisions



Resonance	ρ^0	K^{*0}	$\Sigma^{*\pm}$	$\Lambda(1520)$	Ξ^{*0}	ϕ
Lifetime (fm/c)	1.3	4.16	5.5	12.6	21.7	46.2



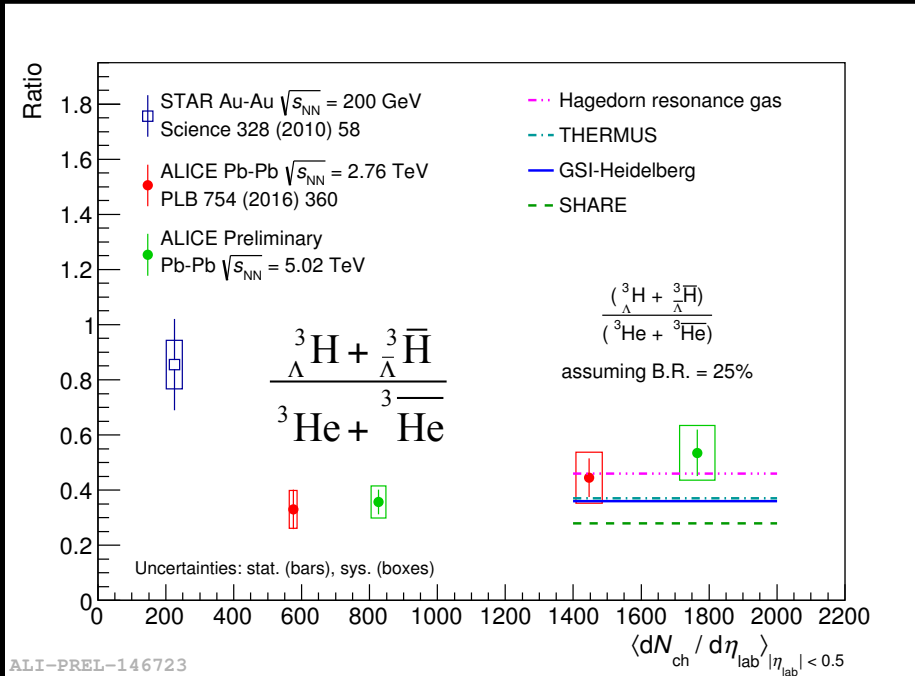
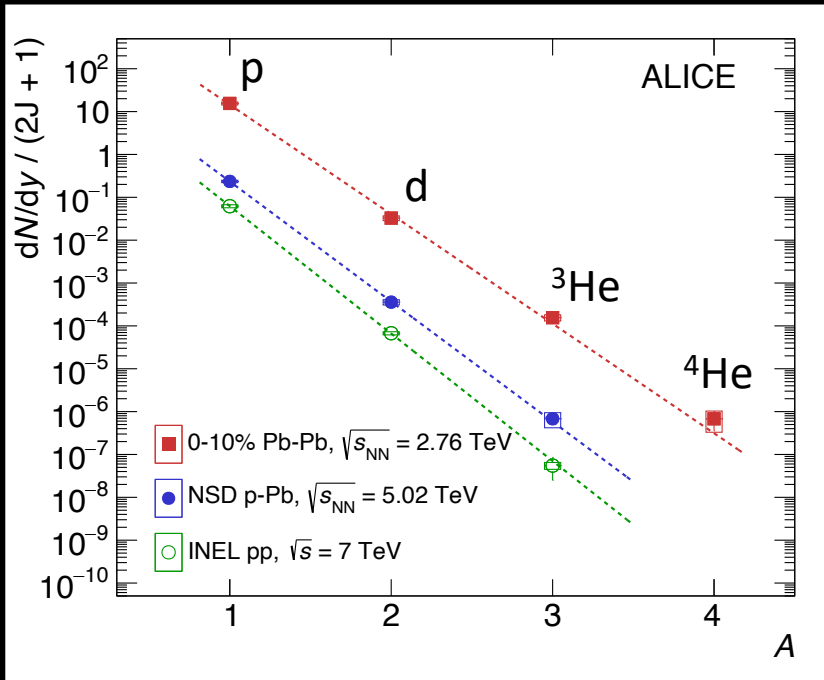
- Relative suppression of ρ^0 , K^{*0} , $\Lambda(1520)$ with increasing multiplicity
- Σ^*/Λ , Ξ^*/Ξ , ϕ/K is independent of multiplicity
- Similar trend seen in all collision systems
- EPOS3 + UrQMD describes the trend of data

ρ^0 : Phys. Rev. C99, (2019) 064901
 K^{*0} : Phys. Rev. C95, (2017) 064606
 $\Lambda(1520)$: Phys. Rev. C99, (2019) 024905
 STAR, Phys. Rev. C78 (2008) 044906
 STAR, Phys. Rev. Lett. 97 (2006) 132301
 ϕ : Phys. Rev. C91 (2015) 024609
 Σ^*, Ξ^* : Eur. Phys. J. C 77 (2017) 389

→ Dominance of rescattering over (re)combination in hadronic phase

Nuclei production in pp, p-Pb and Pb-Pb

p-Pb: Phys. Lett. B 800 (2019) 135043

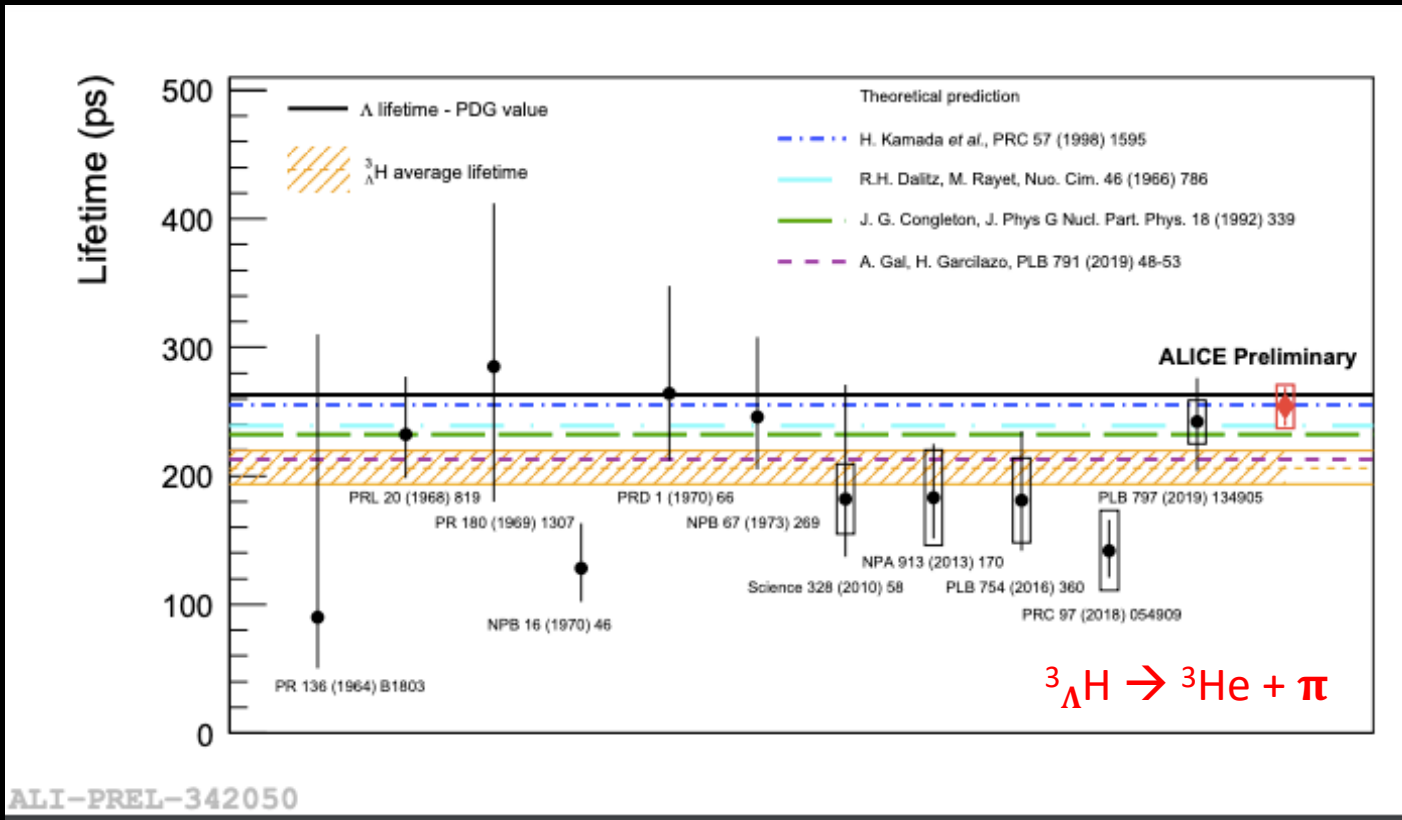


- Exponential decrease in nuclei rate described by thermal model
- Nuclei production rate decreases by factor of ~ 300 (Pb-Pb), ~ 600 (p-Pb) and ~ 1000 (pp) for each additional nucleon
- $^3\Lambda$ production consistent with thermal model (binding energy $\sim 0.13 \text{ MeV} \ll T_{ch}$)
→ Production mechanisms: thermal vs coalescence?

pp: Phys. Rev. C97 (2018) 024615

Pb-Pb: Nucl. Phys. A 971 (2018) 1

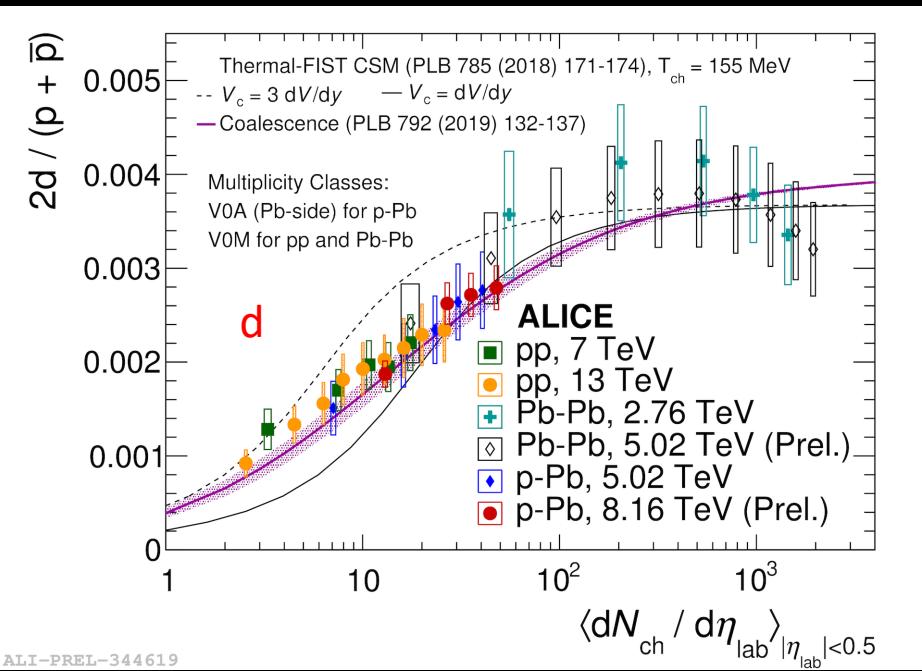
Hypertriton lifetime



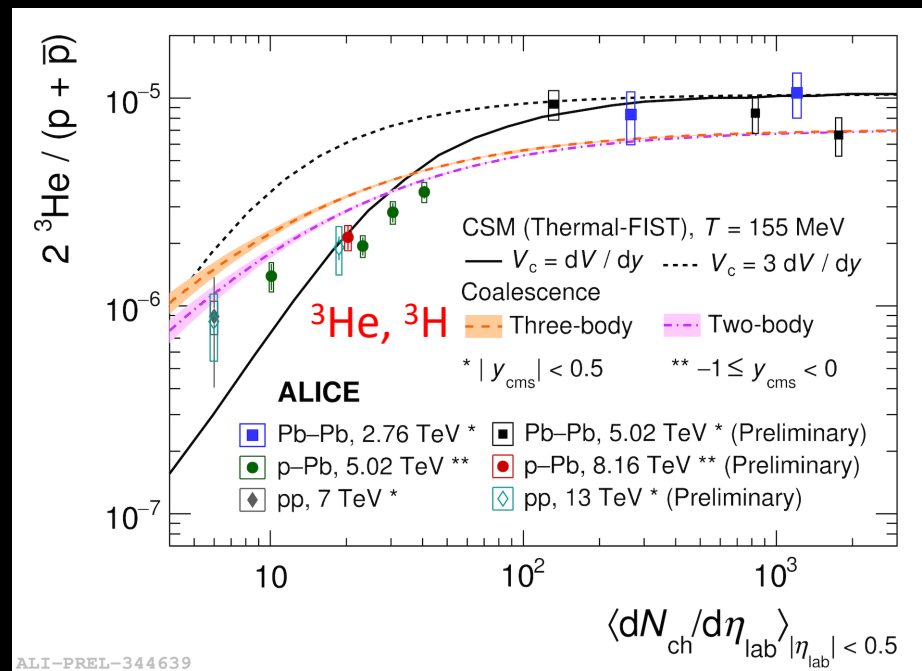
ALI-PREL-342050

- The most precise measurement of hypertriton lifetime
- Two body 3H decay channel has been used
- 3H lifetime consistent with the free Λ lifetime (not included in the average)
 \rightarrow binding energy ~ 0.13 MeV
- Large discrepancy between recent World results

Formation of light nuclei



ALI-PREL-344619



ALI-PREL-344639

- Increase from pp to peripheral Pb-Pb
- No centrality dependence in high multiplicity Pb-Pb
- Data described qualitatively by coalescence and thermal models

→ Production mechanisms: thermal vs coalescence?

Thermal- FIST CSM: V. Vovchenko et al., Phys. Lett. B 785 (2018) 171

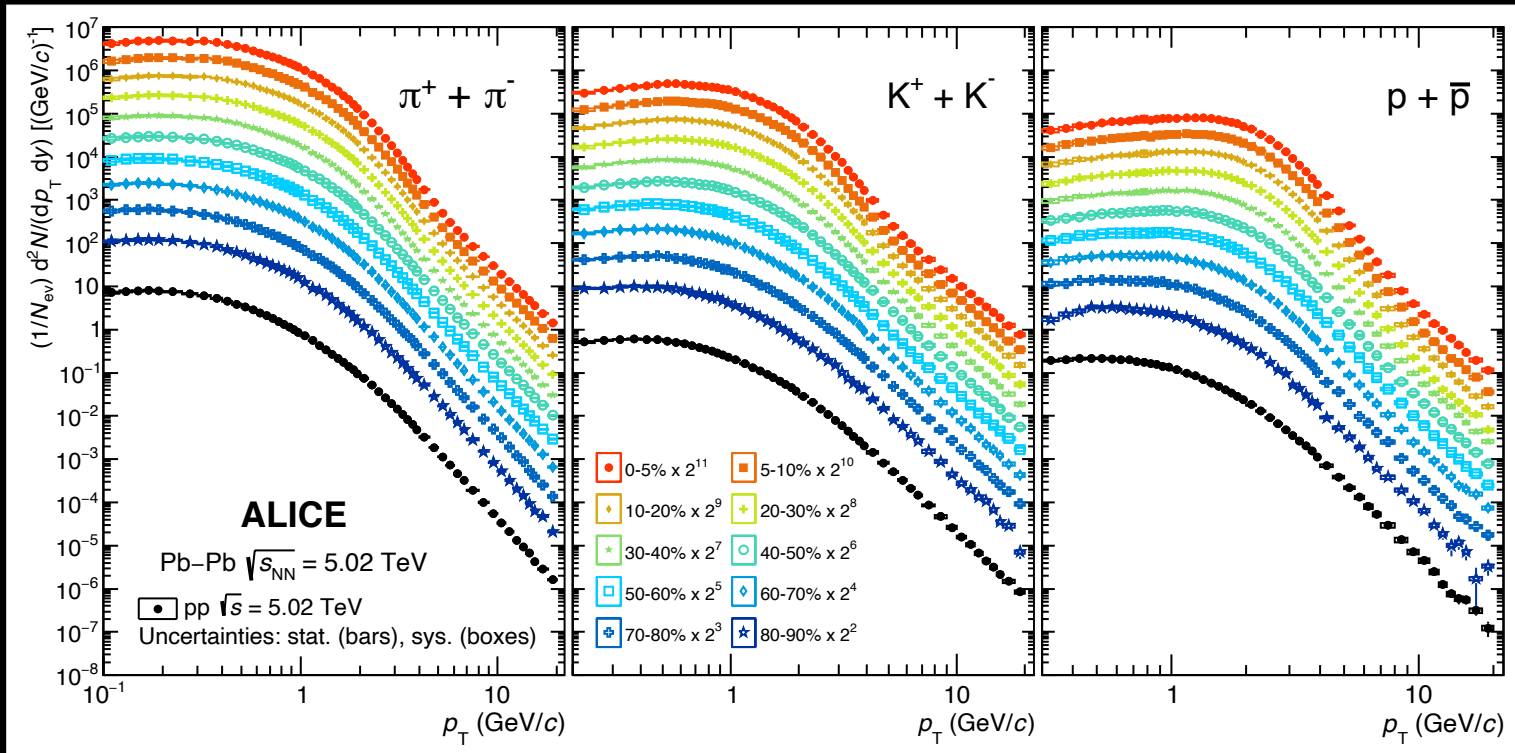
Coalescence: K.-J. Sun et al., Phys. Lett. B 792 (2019) 132

SPECTRA

Transverse momentum spectra of charged π , K and p in Pb-Pb

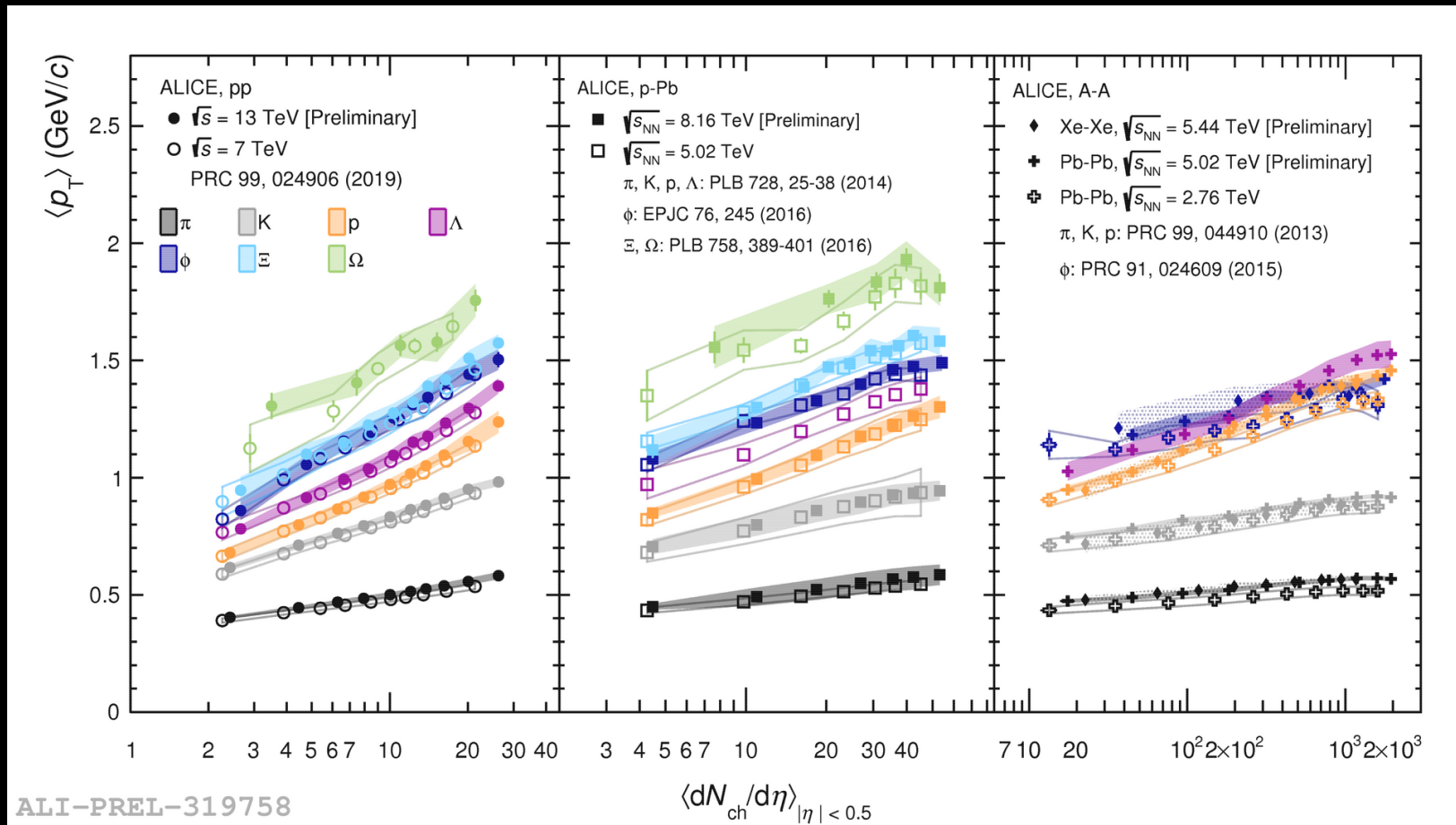


Phys. Rev. C 101, 044907 (2020)



- Particle identification with different analysis techniques: ITS, TPC, TOF, HMPID and topological identification of decaying charged kaons
- Mass dependent hardening of the spectra with increasing centrality
→ Collective radial expansion

$\langle p_T \rangle$ vs centrality of hadrons in pp, p-Pb, Pb-Pb and Xe-Xe



- $\langle p_T \rangle$ increases with increasing centrality and mass
- Larger increase in smaller systems
→ Collective radial expansion

pp 13 TeV: arXiv:2005.11120
Xe-Xe 5.44 TeV: arXiv:2101.03100
Pb-Pb 5.02 TeV: PRC 101, 044907 (2020)

Blast-Wave fit to hadron p_T spectra

$$E \frac{d^3 N}{d p^3} \propto \int_0^R m_T I_0 \left(\frac{p_T \sinh(\rho)}{T_{\text{Kin}}} \right) K_1 \left(\frac{m_T \cosh(\rho)}{T_{\text{Kin}}} \right) r dr$$

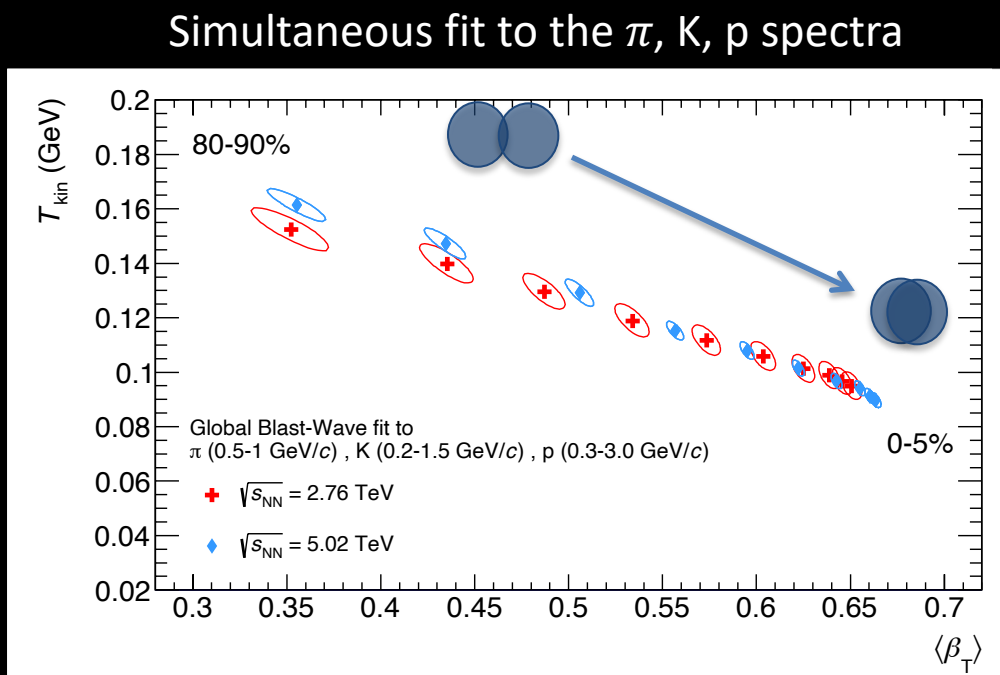
$$m_T = \sqrt{m^2 + p_T^2} \quad \rho = \tanh^{-1}(\beta_T) \quad \beta_T = \beta_s \left(\frac{r}{R} \right)^n$$

Schnedermann, Sollfrank and Heinz Phys. Rev. C 48, 2462

Simplified hydrodynamic model with 3 parameters:

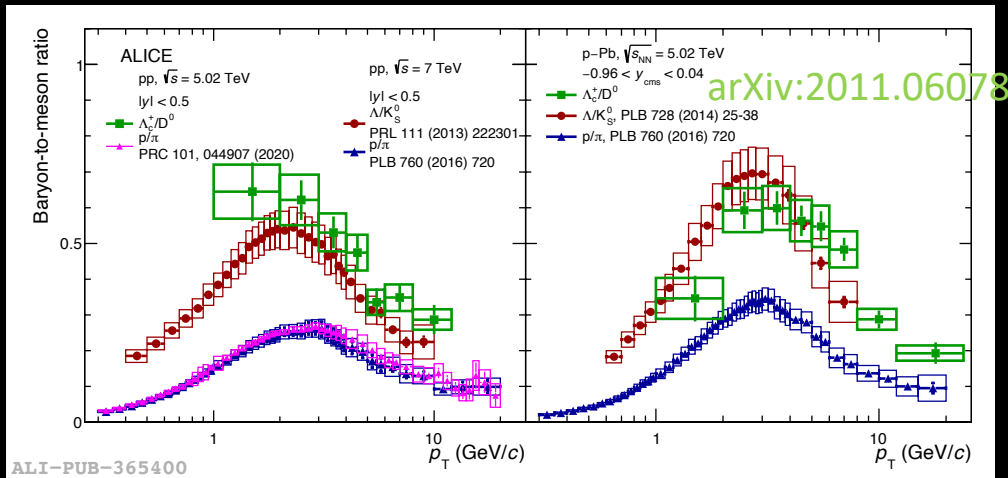
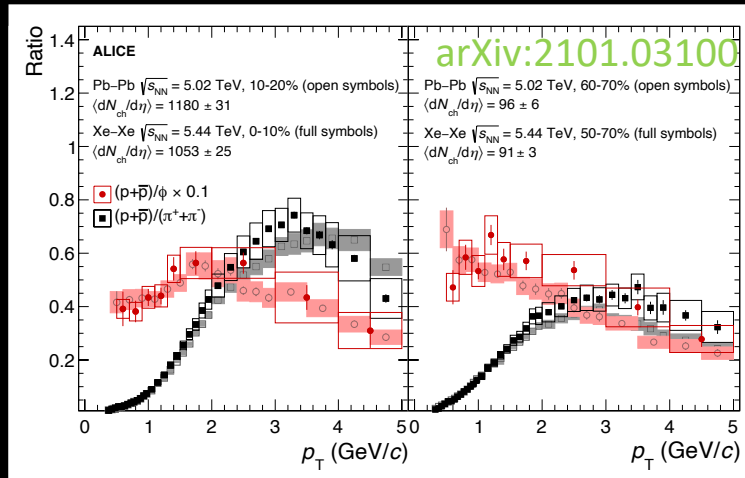
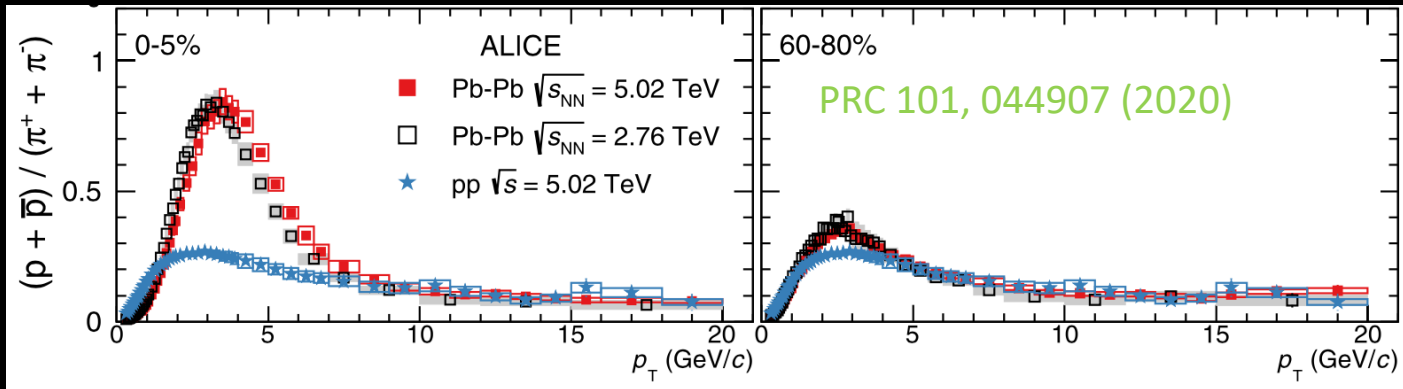
- β_T - radial expansion velocity
- T_{kin} – kinetic freeze-out temperature
- n – velocity profile

Phys. Rev. C 101, 044907 (2020)



- $\langle \beta_T \rangle$ reaches $\sim 0.65c$ in central Pb-Pb collisions
- T_{kin} decreases with collision centrality

Baryon-to-meson ratios

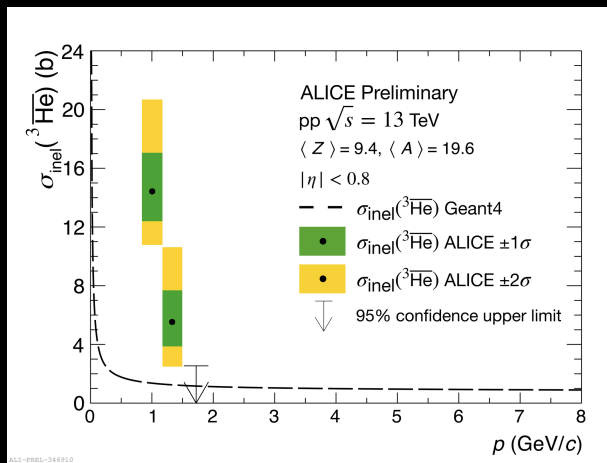
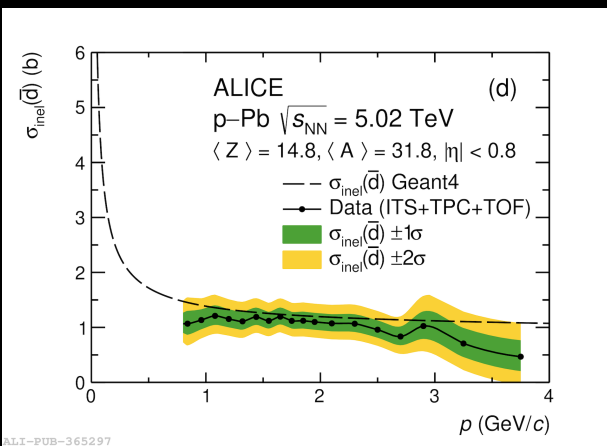
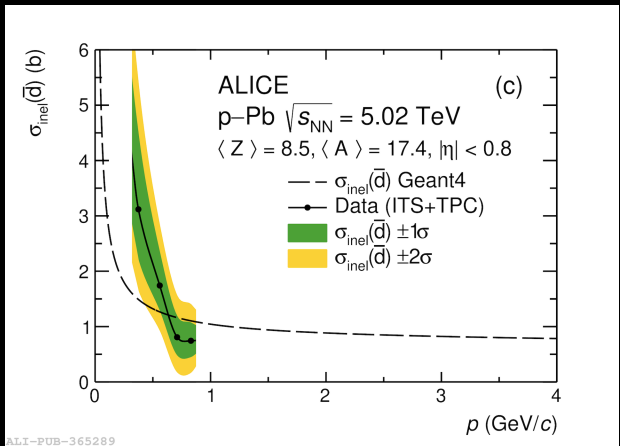


- Similar trends independent of collision system for the same multiplicity
- Λ_c^+ / D^0 show similarities with those for light-flavor p/π and Λ_c^+ / K_s^0
 → hint for the common production mechanism of light- and heavy-flavor baryons
 (coalescence vs. fragmentation)

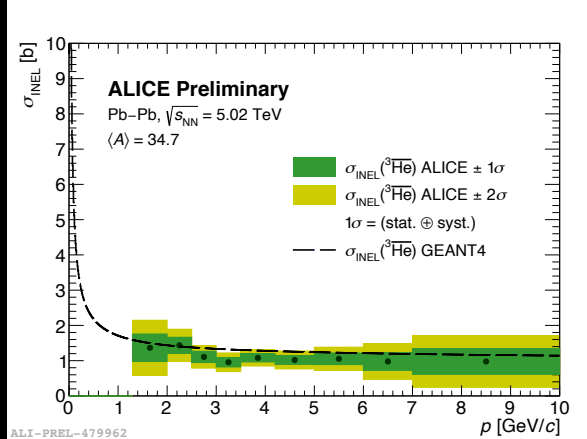
Antinuclei interaction cross sections



Phys. Rev. Lett. 125 (2020) 162001



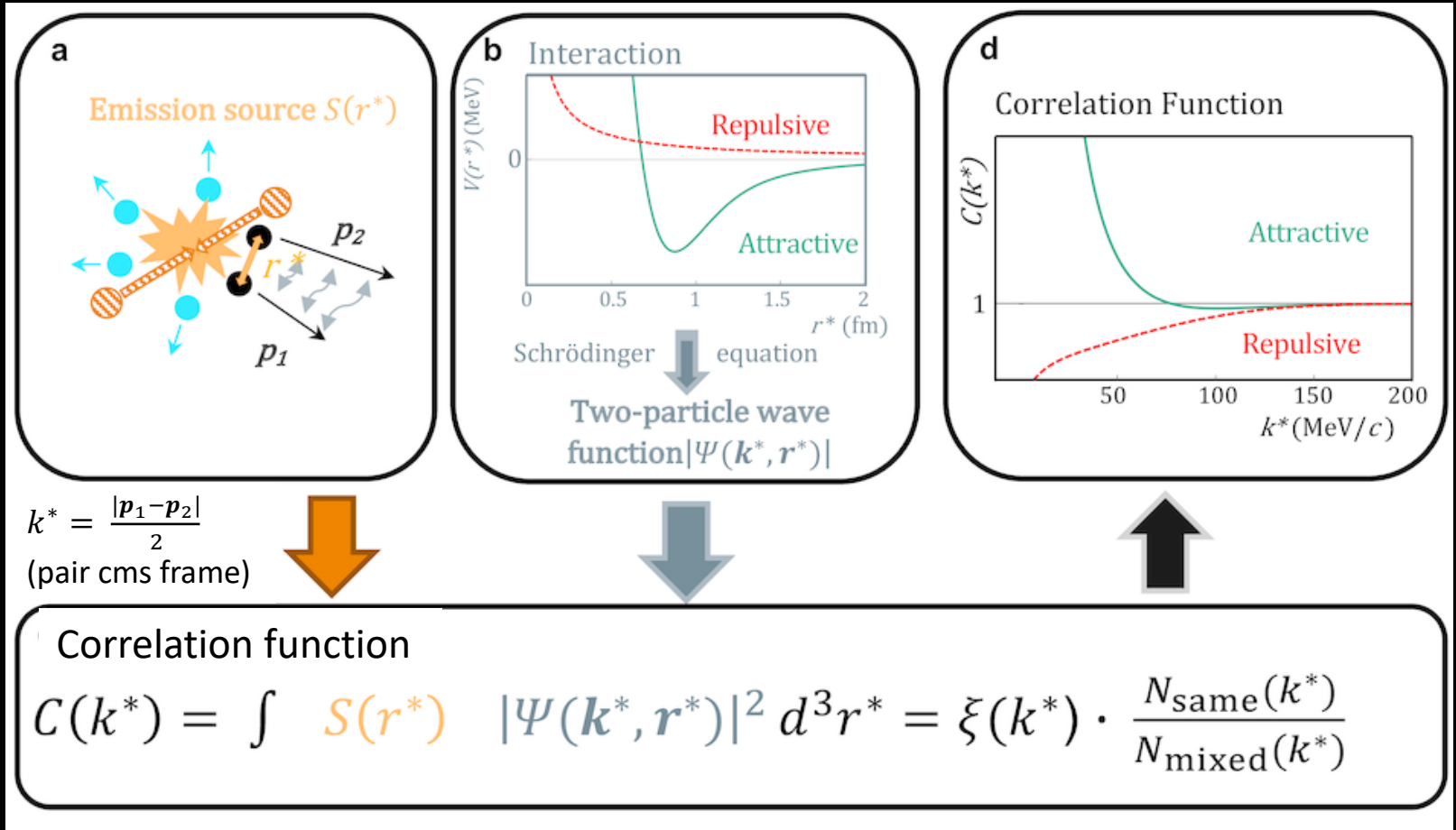
- Studies relevant for understating anti-nuclei absorption in the galactic medium (dark matter searches)
- First measurement of anti-deuteron and anti- ${}^3\text{He}$ INEL cross section at low momentum
- ALICE detector material used as target to study anti-nuclei absorption





FEMTOSCOPY CORRELATIONS

Femtoscopy correlations to study stable and unstable hadron interactions

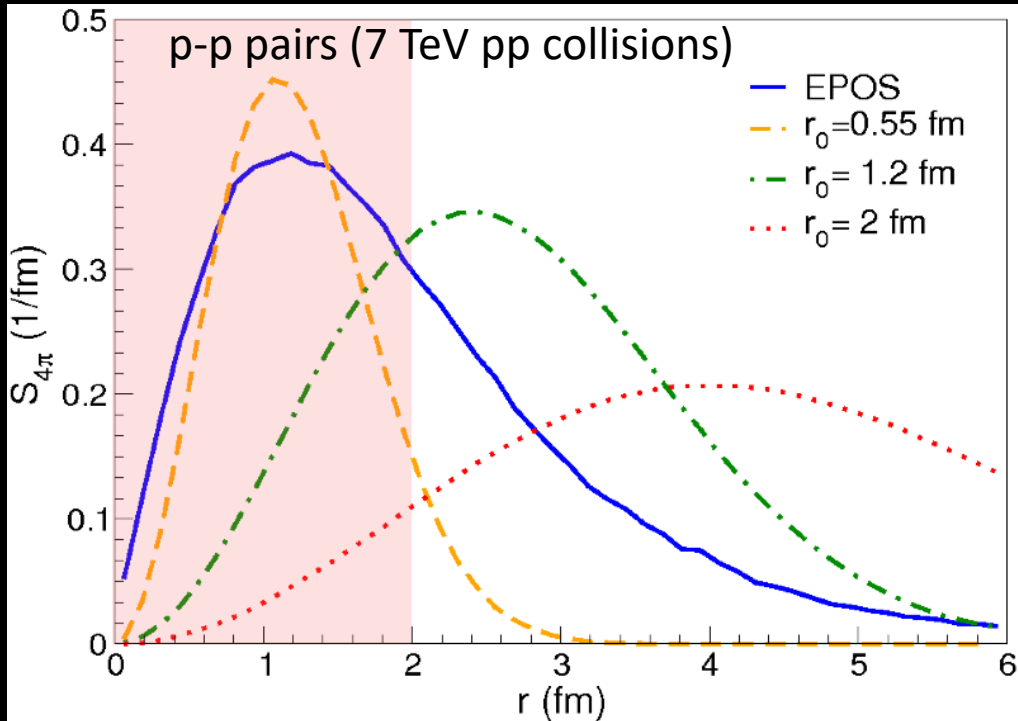


- Origin of correlations: quantum interference, resonances, conservation laws or final-state interactions
- Final-state interactions dominate at small k^*

Pioneering by HADES Coll.
Phys. Rev. C 94, 025201 (2016)

Femtoscopy in small systems

CATS, D. Mihaylov et al., Eur. Phys. J. C78 (2018) 394



Gaussian emission source:

$$S(r^*) = \frac{1}{(4\pi r_0^2)^{3/2}} \exp\left(-\frac{r^{*2}}{4r_0^2}\right)$$

Pair emission probability:

$$S_{4\pi}(r^*) = 4\pi r^2 S(r^*)$$

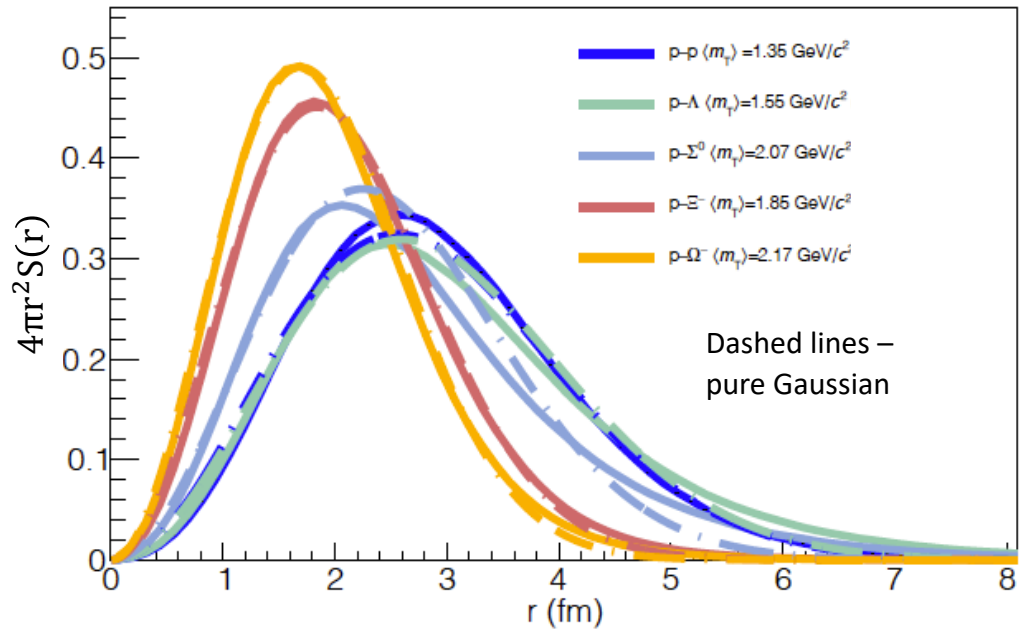
EPOS model predicts non-Gaussian emission source

T. Pierog et al. PRC 92 (2015) 034906

- A lot of pairs is emitted from the source at distance below $\sim 2 \text{ fm}$ (typical range of strong interaction)
- Small particle emission source in pp and p-Pb collisions is essential to study the strong interaction!

Common baryon source

Source using a Gaussian core plus resonances



ALICE PLB 811 (2020) 135849

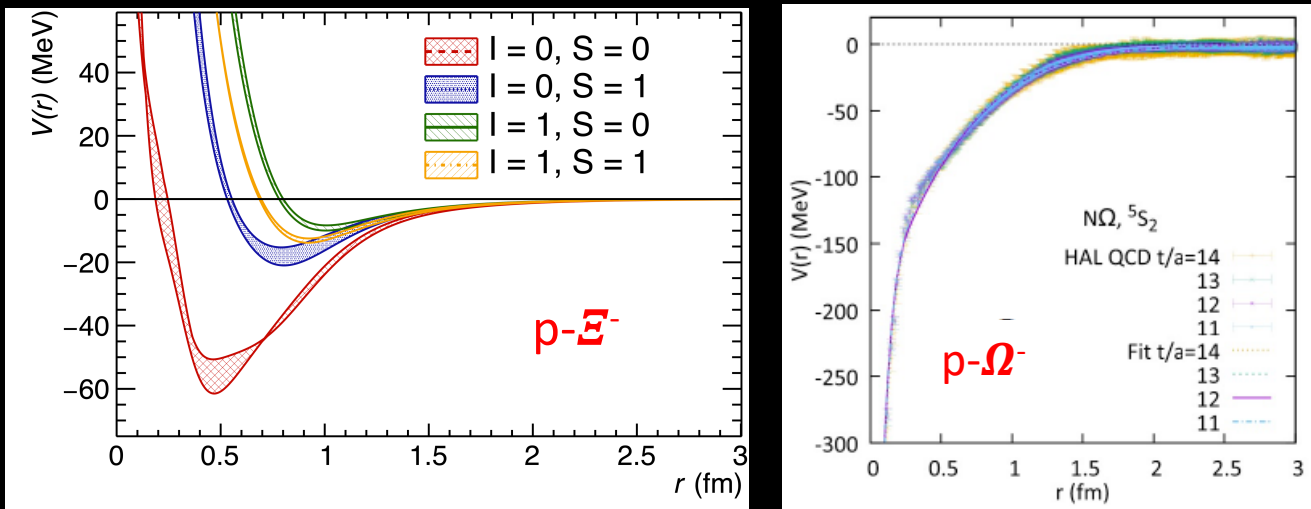
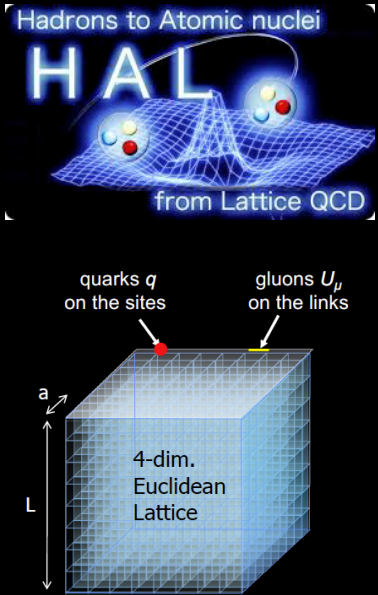
Pair	r_{Core} [fm]	r_{Eff} [fm]
p-p	1.1	1.2
p- Λ	1.0	1.3
p- Σ^0	0.87	1.02
p- Ξ^-	0.93	1.02
p- Ω^-	0.86	0.95

$$S(r^*) = G(r^*, r_{core}(m_T)) = \frac{1}{(4\pi r_{core}^2)^{3/2}} \exp\left(-\frac{r^{*2}}{4r_{core}^2}\right) \otimes E(r^*, M_{res}, \tau_{res}, p_{res})$$

- Emission source for heavier pairs using p-p correlation function plus resonances
- Gaussian source with $r_{\text{eff}} = 1.02 \pm 0.05$ (0.95 ± 0.06) fm used for the p- Ξ^- (p- Ω^-) emission

The strong interaction for p- Ξ and p- Ω on lattice

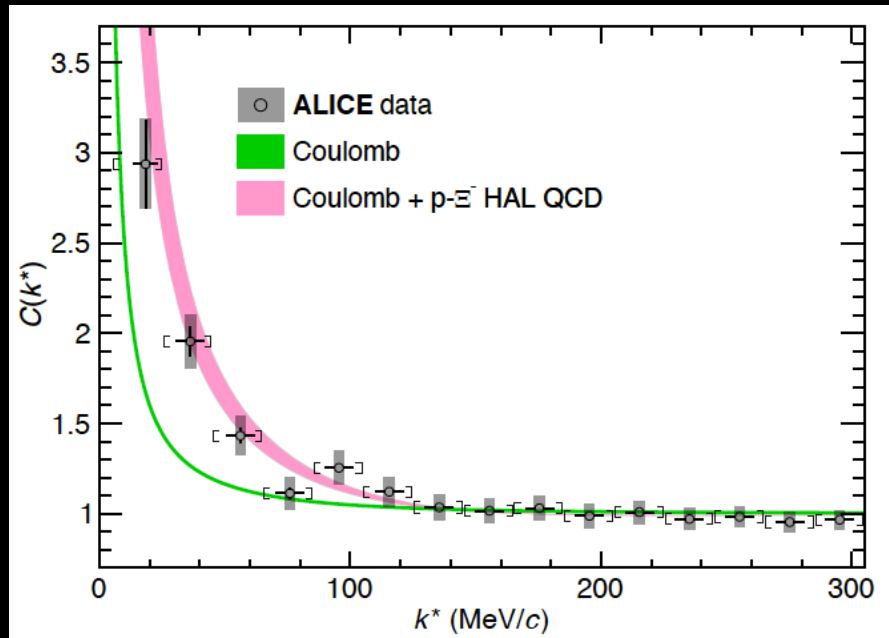
HAL QCD Coll., NPA 998 (2020) 121737, PLB 792 (2019) 284



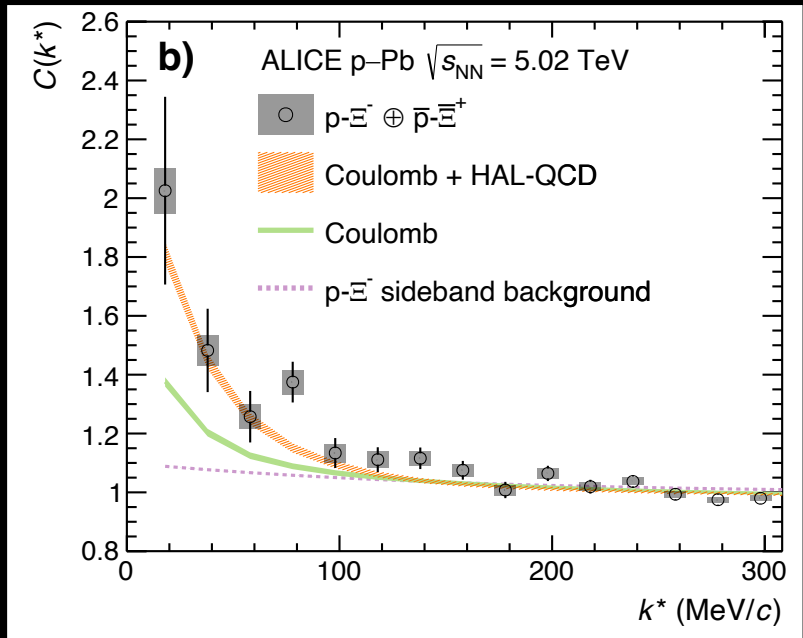
- p- Ξ interaction in four channels: isospin ($I = 0, 1$) and spin ($S=0,1$)
 - Attractive with repulsive core at small distances
- p- Ω interaction in 5S_2 ($I=1/2, S=2$) channel
 - Attractive in the whole range
 - After inclusion Coulomb interaction prediction of bound state with binding energy ~ 2.5 MeV
- p- Ω interaction in 3S_1 channel does not include yet inelastic channels (e.g. $p\Omega \rightarrow \Lambda\Xi$)

p- Ξ correlation function in pp and p-Pb

Nature 588 (2020) 232



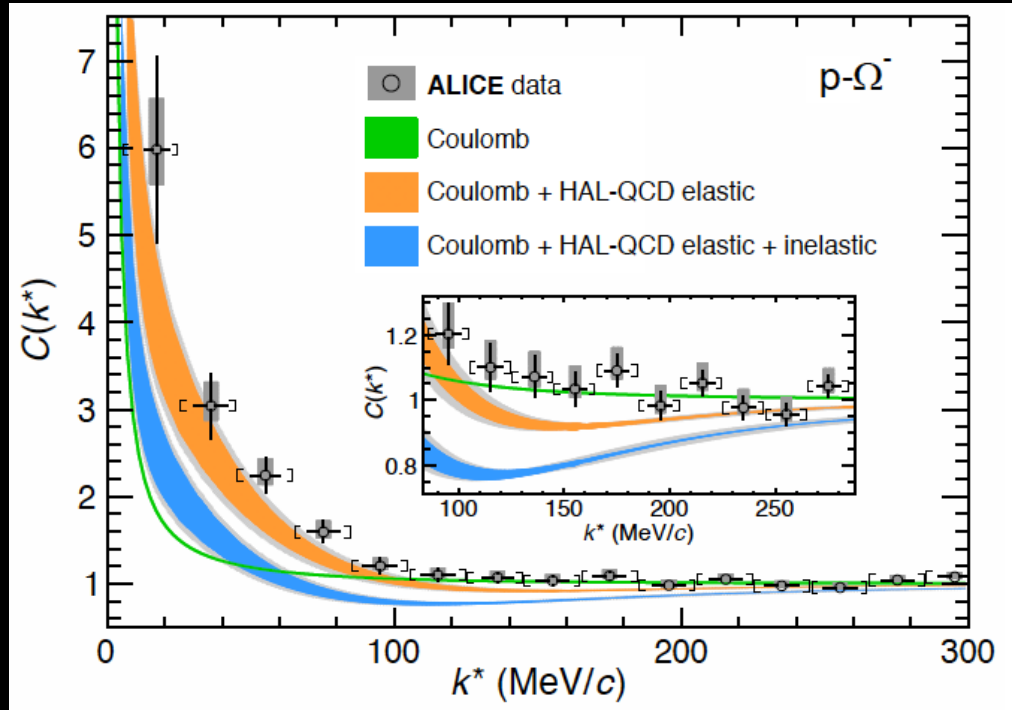
Phys. Rev. Lett. 123, 112002 (2019)



- p- Ξ interaction is attractive
- No indication of bound state in data
- p- Ξ interaction stronger than Coulomb \rightarrow observation of strong interaction
- Coulomb + HAL QCD in agreement with p- Ξ measurements

$p\text{-}\Omega$ correlation function in pp at 13 TeV

Nature 588 (2020) 232



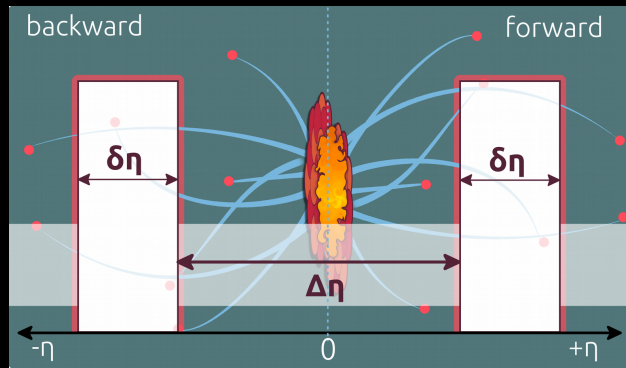
- $p\text{-}\Omega$ interaction is attractive
- No indication of bound state in data
- $p\text{-}\Omega$ interaction stronger than Coulomb → observation of strong interaction
- Calculations underestimate $p\text{-}\Omega$ measurements for both cases tested for missing $p\text{-}\Omega$ inelastic channels in 3S_1 state
 - Inelastic channel dominated by absorption
 - Neglecting inelastic channel

CORRELATIONS AND FLUCTUATIONS

Forward-backward correlations with strongly intensive quantity Σ



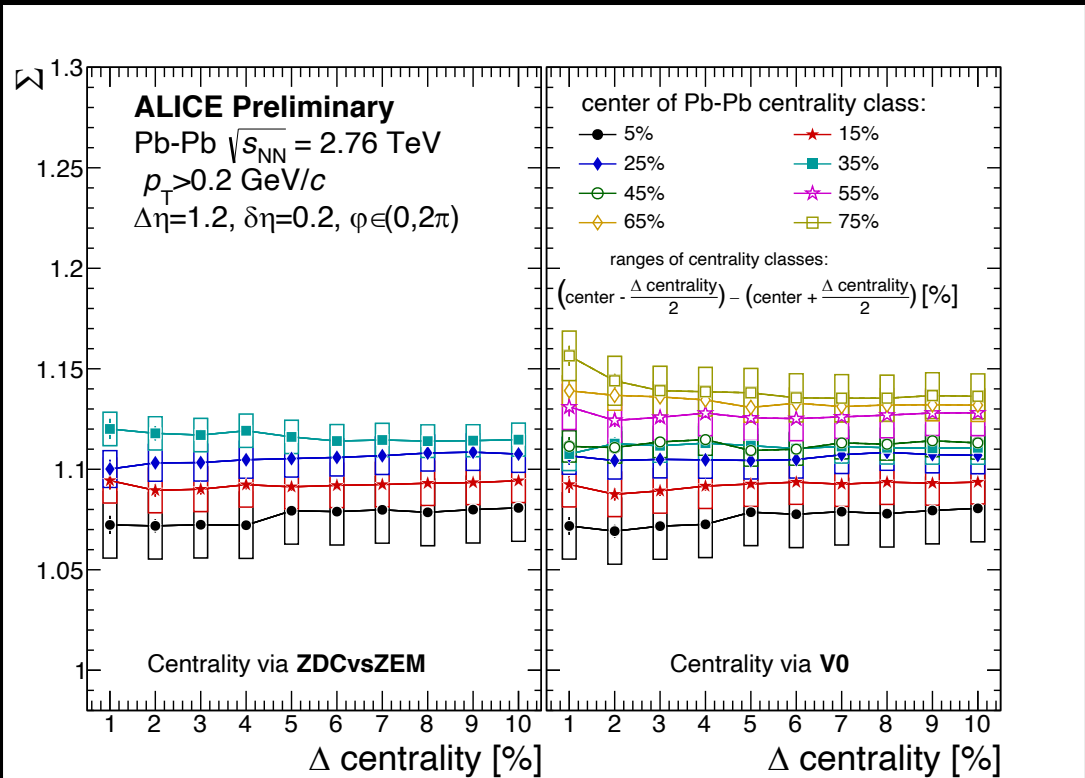
Σ provides information on the early collision dynamics



$$\Sigma = \frac{1}{\langle n_B \rangle + \langle n_F \rangle} [\langle n_F \rangle \omega_B + \langle n_B \rangle \omega_F - 2 \text{Cov}(n_F, n_B)]$$

$$\omega_B(F) = \frac{\text{Var}(n_{B(F)})}{\langle n_{B(F)} \rangle}$$

M. Ga dzicki and M. I. Gorenstein,
PRC84 (2011) 014904



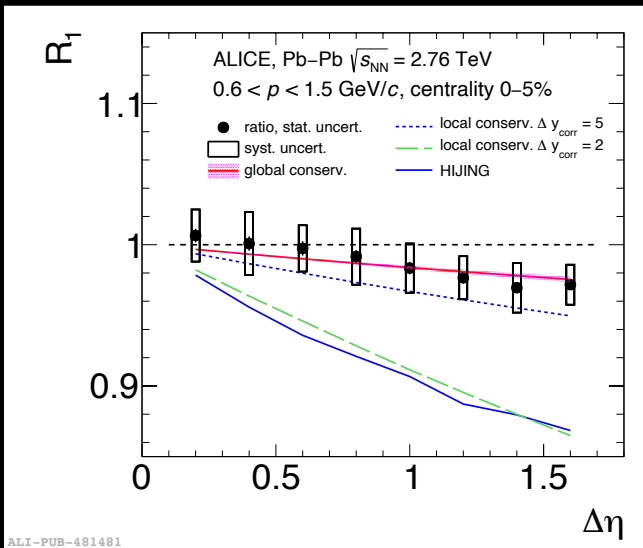
- Σ is independent from event centrality estimator and width of the centrality interval

Net-proton fluctuations in Pb-Pb at 2.76 TeV

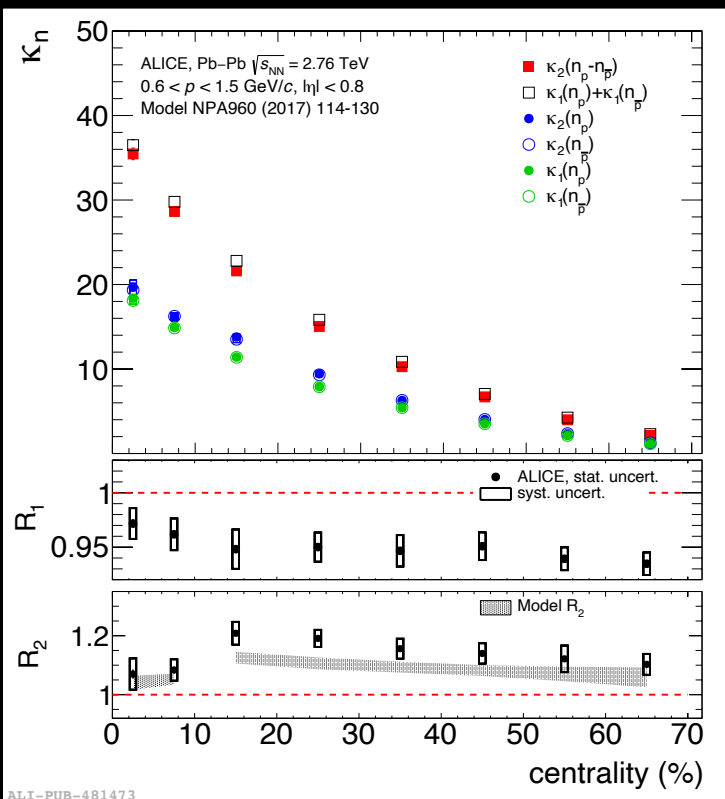
$$\kappa_1(\Delta n_B) = \sum_{\Delta n_B=-\infty}^{\infty} \Delta n_B P(\Delta n_B) = \langle \Delta n_B \rangle,$$

$$\kappa_2(\Delta n_B) = \sum_{\Delta n_B=-\infty}^{\infty} (\Delta n_B - \langle \Delta n_B \rangle)^2 P(\Delta n_B) = \langle (\Delta n_B - \langle \Delta n_B \rangle)^2 \rangle$$

$$R_1 = \kappa_2(n_p - n_{\bar{p}}) / \langle n_p + n_{\bar{p}} \rangle, \quad R_2 = \kappa_2(n_p) / \langle n_p \rangle$$



Phys. Lett. B 807 (2020) 135564



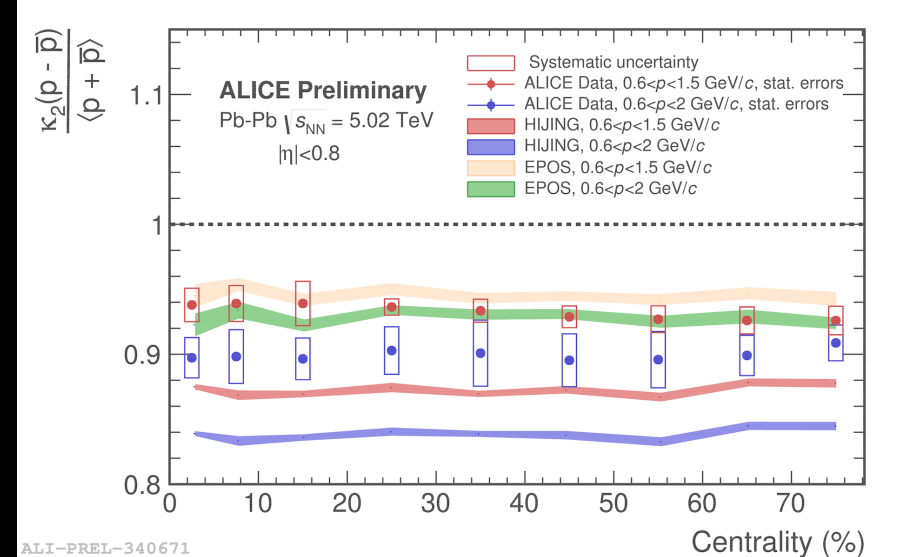
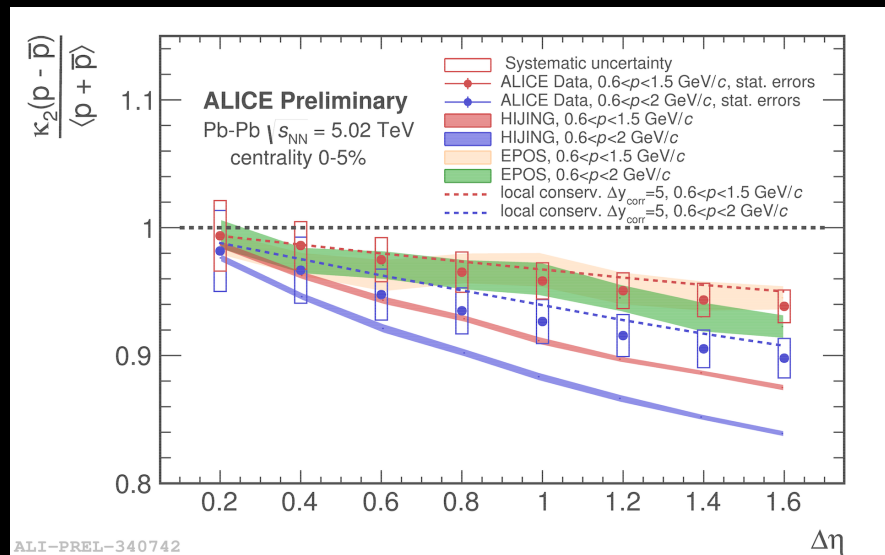
- Event-by-event baryon number conservation leads to subtle long-range correlations arising from very early interactions in the collisions
- Experimental tests of lattice QCD predictions on second and higher order cumulants of net-baryon distributions → critical behavior near QCD phase boundaries

Net-proton fluctuations in Pb-Pb at 5.02 TeV

$$\kappa_1(\Delta n_B) = \sum_{\Delta n_B=-\infty}^{\infty} \Delta n_B P(\Delta n_B) = \langle \Delta n_B \rangle,$$

$$\kappa_2(\Delta n_B) = \sum_{\Delta n_B=-\infty}^{\infty} (\Delta n_B - \langle \Delta n_B \rangle)^2 P(\Delta n_B) = \langle (\Delta n_B - \langle \Delta n_B \rangle)^2 \rangle$$

$$R_1 = \kappa_2(n_p - n_{\bar{p}}) / \langle n_p + n_{\bar{p}} \rangle, \quad R_2 = \kappa_2(n_p) / \langle n_p \rangle$$

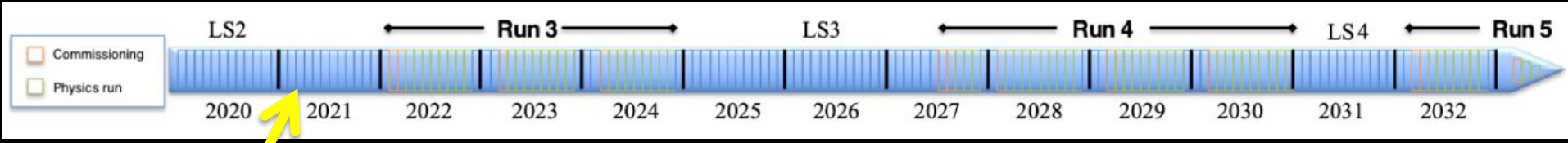


- Event-by-event baryon number conservation leads to subtle long-range correlations arising from very early interactions in the collisions
- Experimental tests of lattice QCD predictions on second and higher order cumulants of net-baryon distributions → critical behavior near QCD phase boundaries

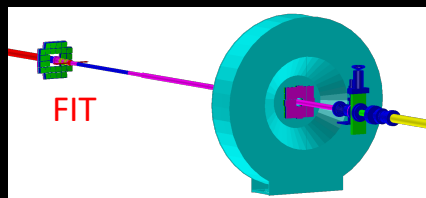
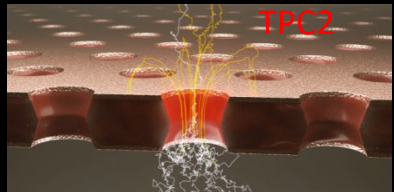
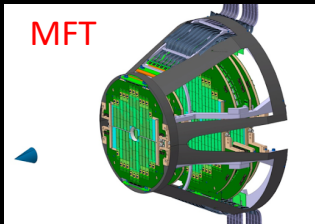
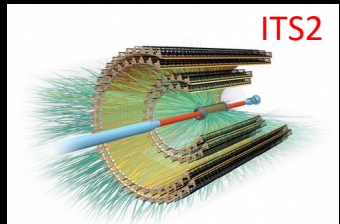
Summary

- Relative to pion particle production is driven by characteristics of final state
- Several mechanisms of hadron and nuclei production: (re)scattering, (re)combination, coalescence etc.
- Collective effects are observed in small and large systems
- The strong interaction between protons and hyperons ($p\text{-}\Xi$ and $p\text{-}\Omega$) is attractive (no indication of bound states)
- Strongly intensive quantities allow for particle correlation studies free from volume size and volume fluctuations
- Baryon number conservation introduces a subtle long-range correlation in net-baryon correlation studies

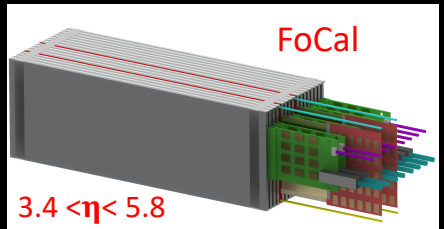
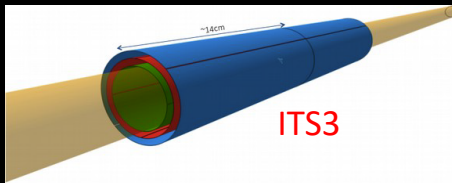
Outlook



LS2: upgrades



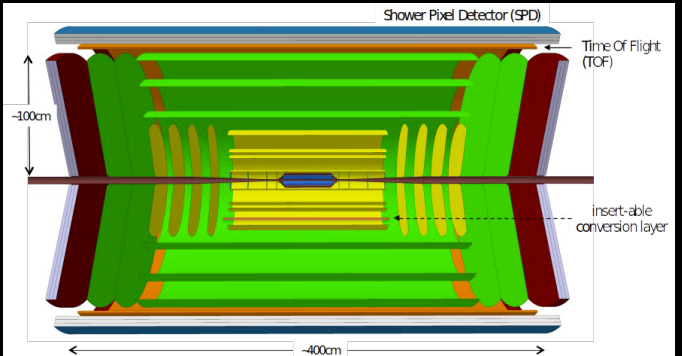
LS3: upgrades



LS4: Future heavy-ion detector arXiv:1902.01211

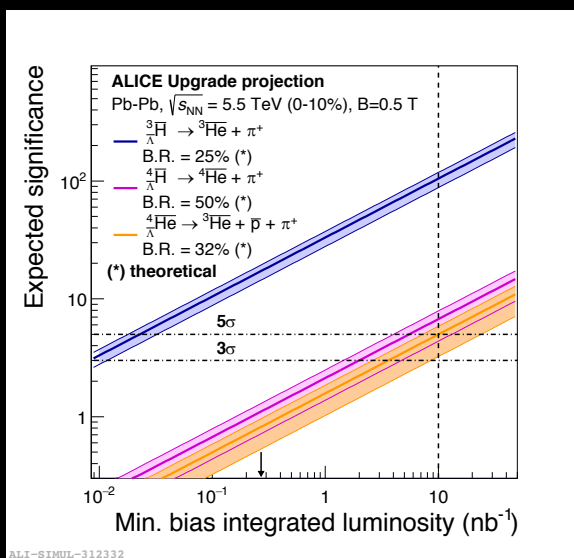
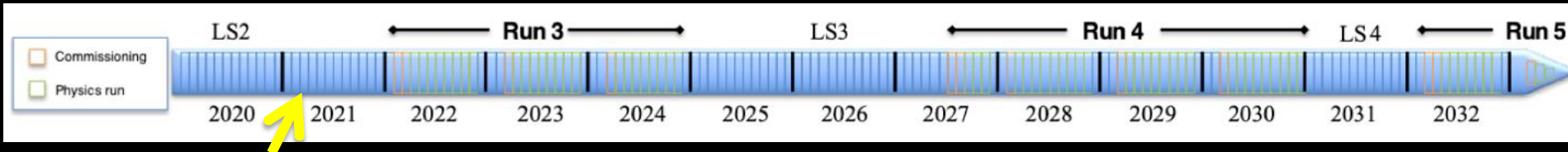
Continuous data taking

- Detector upgrade
- Online-offline computing system upgrade
- Readout electronics and trigger upgrade

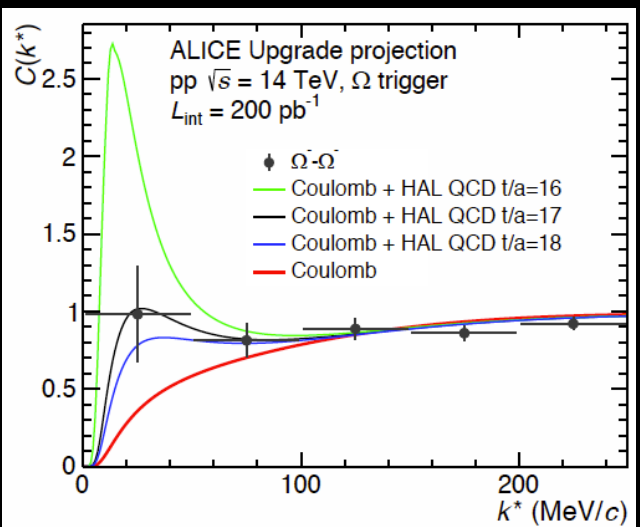


Outlook

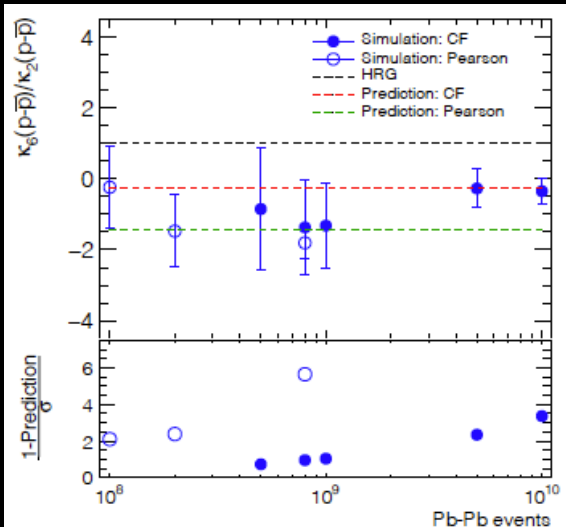
LHC Run3 projected statistic



More than 3σ significance for $\frac{4}{\Lambda}\bar{\text{He}}$



$\Omega - \Omega$ correlations



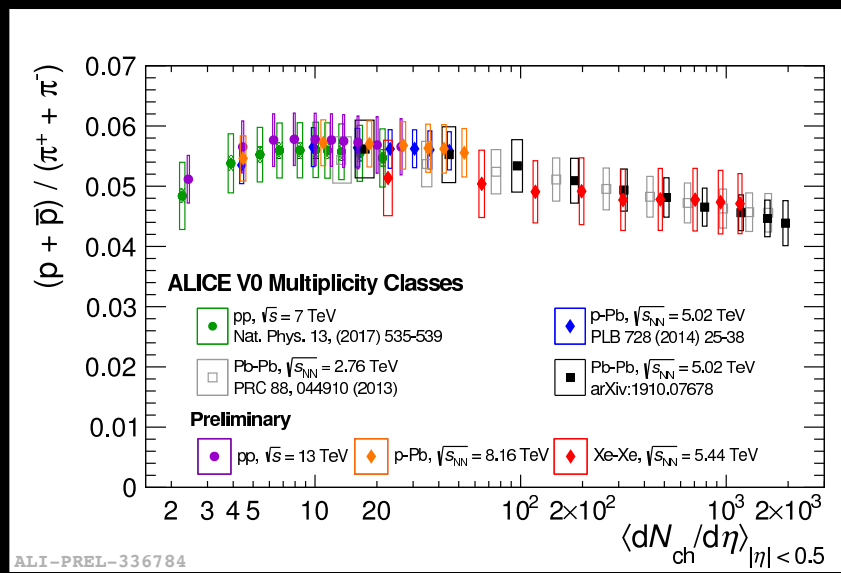
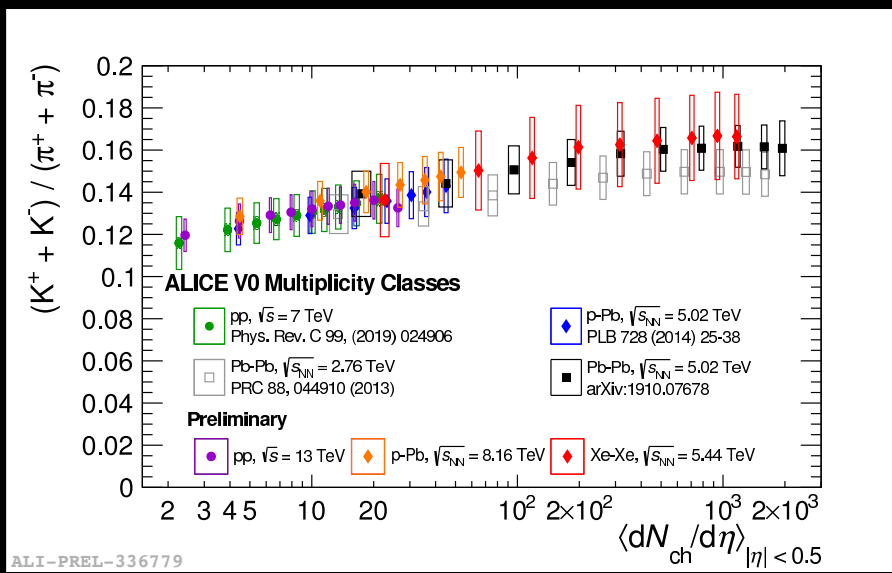
Net-proton 6th order cumulants

THANK YOU FOR YOUR ATTENTION!



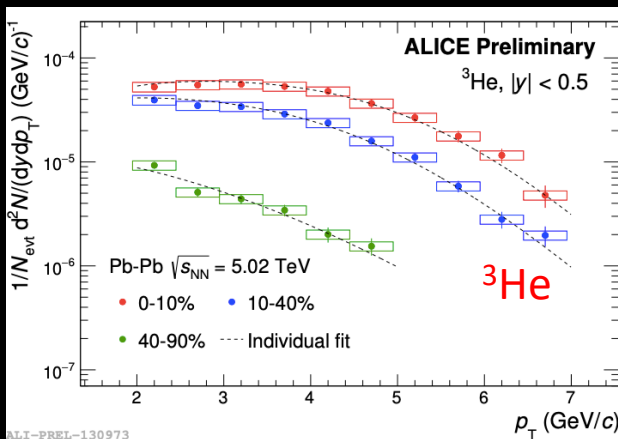
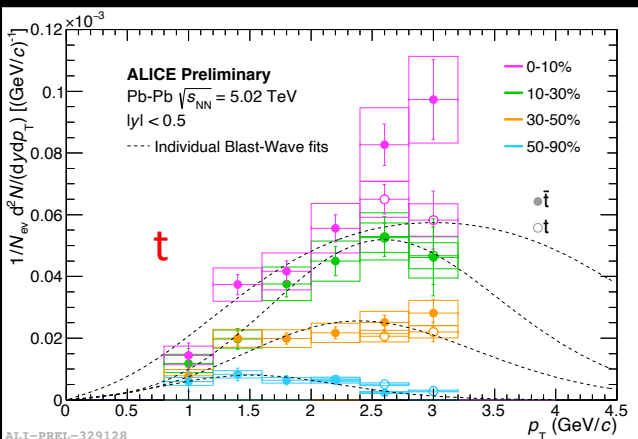
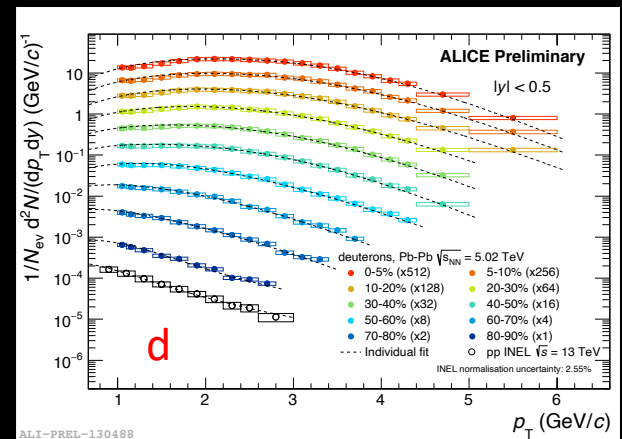
Backup

K/π and p/π in pp, p-Pb, Pb-Pb and Xe-Xe

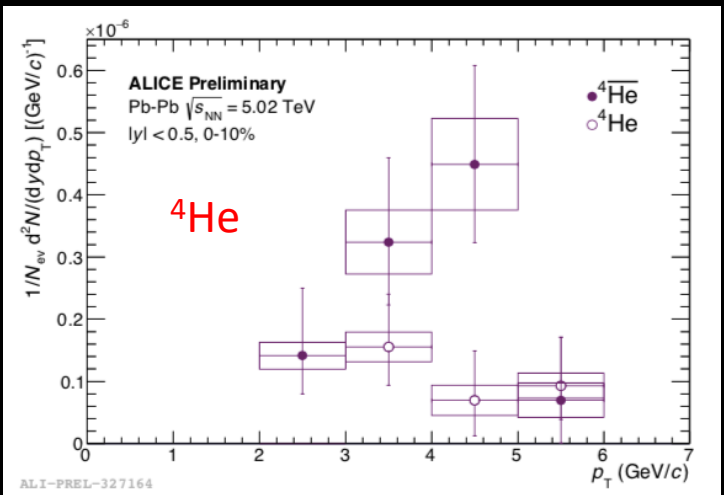


- No significant energy dependence is observed
 - K/π and p/π are consistent for all collision systems at similar multiplicity
- Particle production is driven by the characteristics of final state

(Anti)nuclei p_T spectra in Pb-Pb

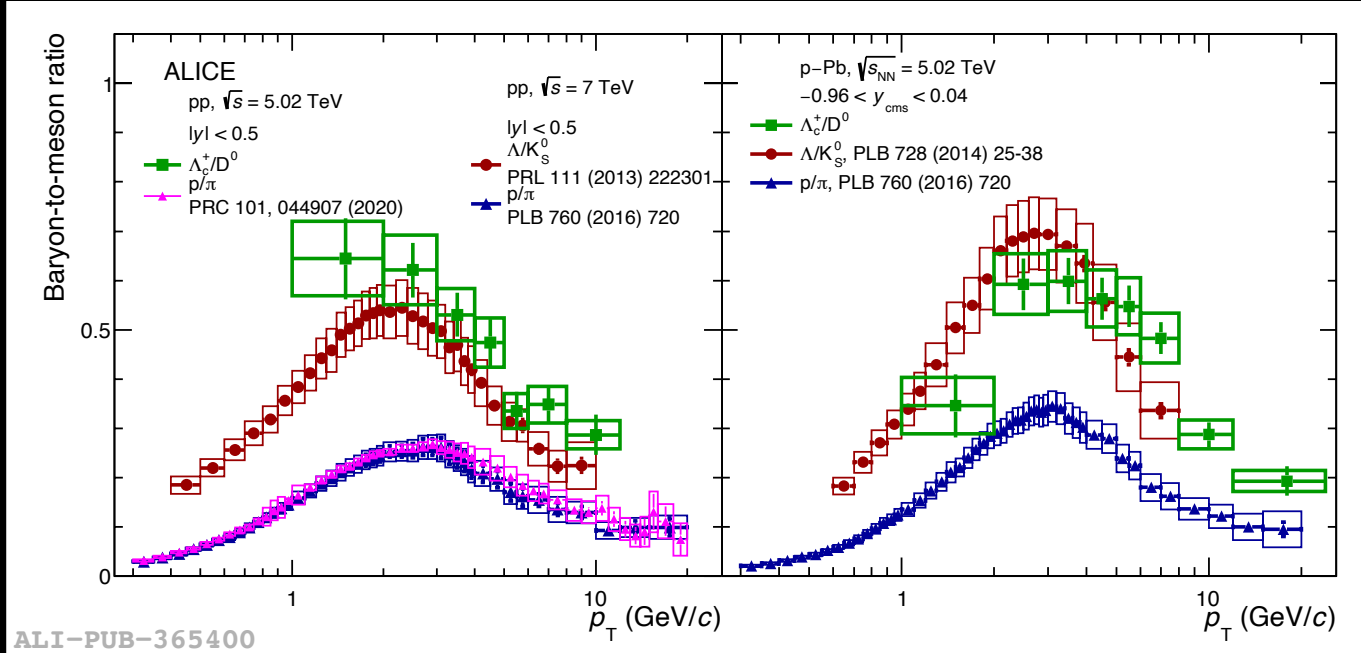


- Light nuclei p_T spectra are modified by radial flow



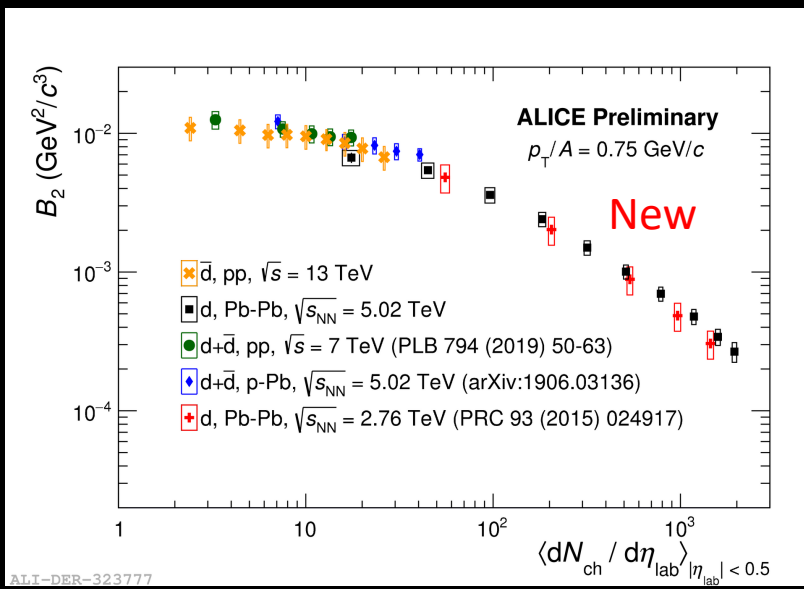
Baryon-to-meson ratios

arXiv:2011.06078



- Baryon-to-meson ratio for Λ_c/\bar{D}^0 show similarities with those for light-flavor p/π and Λ/\bar{K}_s^0
 - hint for the common production mechanism of light- and heavy-flavor baryons (coalescence vs. fragmentation)

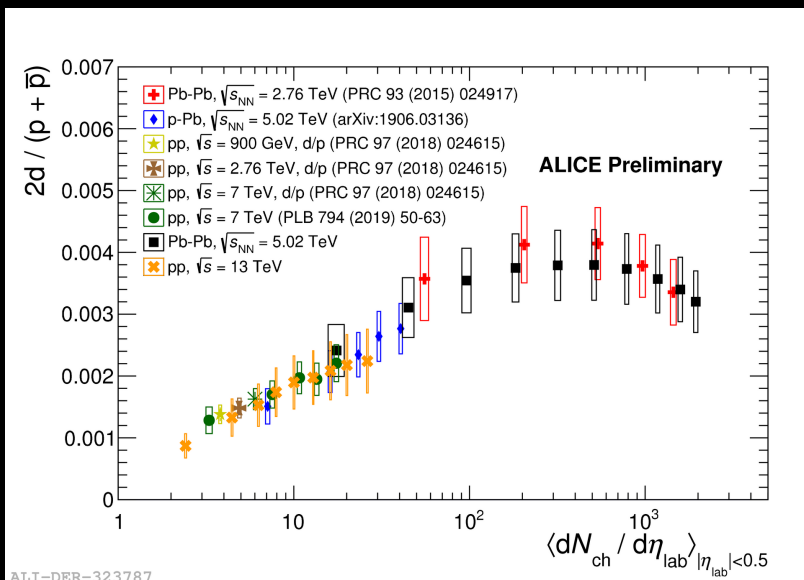
Formation of light nuclei: (anti) deuterons



- Coalescence of baryons close in phase space (A - mass number)

$$E_A \frac{d^3 N_A}{dp_A^3} = B_A \left(E_p \frac{d^3 N_p}{dp_p^3} \right)^A$$

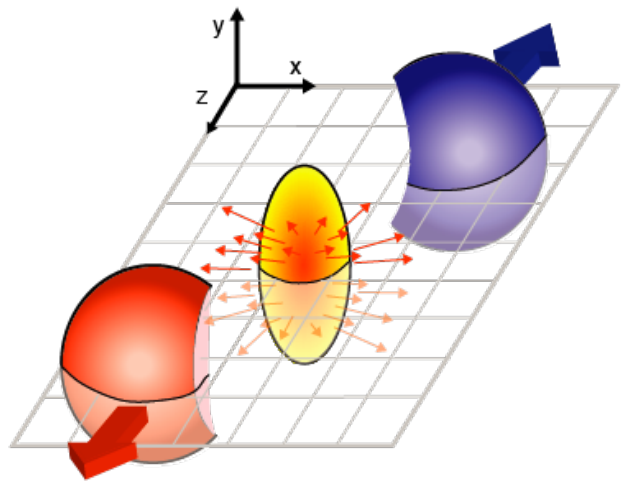
- B_2 shows dependence on multiplicity (no dependence on p_{T})



- d/p vs multiplicity
 - Increase from pp to peripheral Pb-Pb consistent with coalescence model
 - No centrality dependence in high multiplicity Pb-Pb (yields consistent with thermal model)
- Production mechanisms: thermal vs coalescence?

ANISOTROPIC FLOW

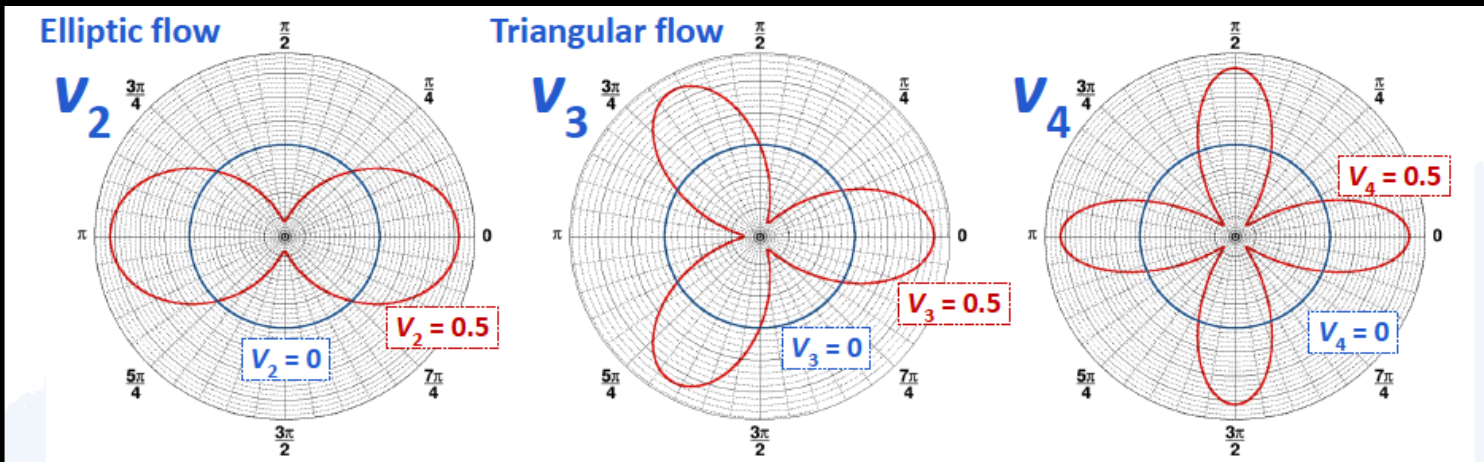
Anisotropic flow



- Strongly interacting system:
spatial anisotropy → momentum anisotropy
- Quantified in terms of Fourier coefficients v_n

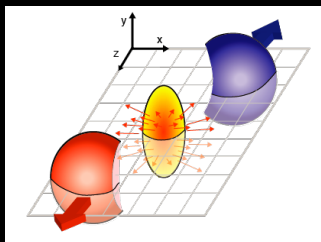
$$E \frac{d^3 N}{d^3 p} = \frac{1}{2\pi} \frac{d^2 N}{p_T dp_T dy} \left(1 + 2 \sum_{n=1}^{\infty} v_n \cos[(\varphi - \Psi_n)] \right)$$

$$v_n(p_T, y) = \langle \cos[n(\varphi - \Psi_n)] \rangle$$



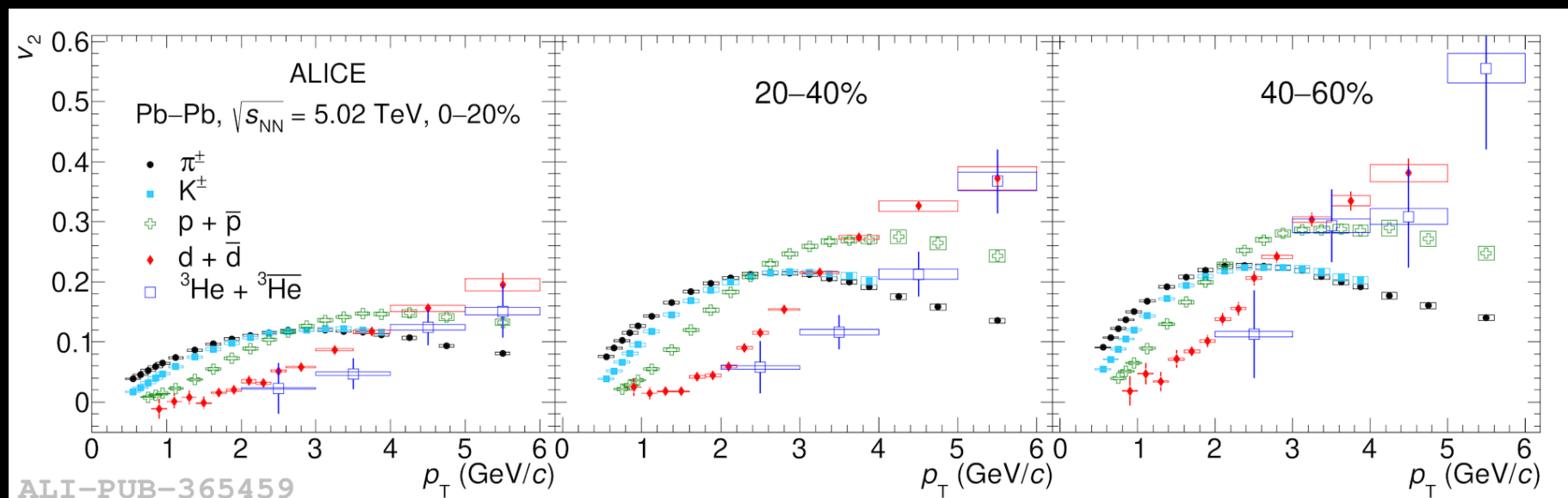
Hadron and nuclei v_2 in Pb-Pb

Phys. Rev. C 102 (2020) 055203



$$f(\varphi) = \frac{1}{2\pi} \left[1 + 2 \sum_{n=1}^{\infty} v_n \cos[n(\varphi - \Psi_n)] \right]$$

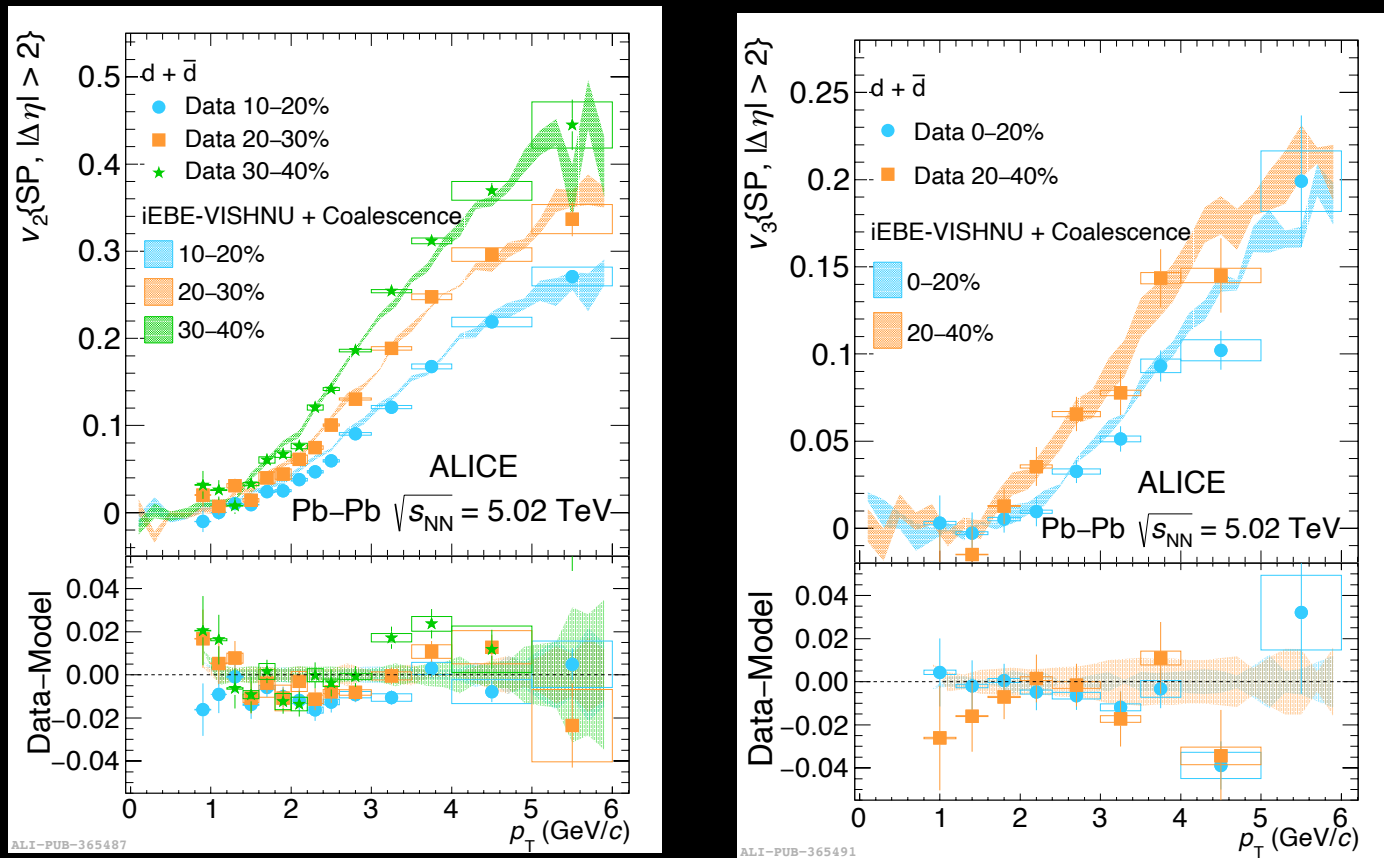
$$v_n(p_T, y) = \langle \cos[n(\varphi - \Psi_n)] \rangle$$



- $p_T < 2$ GeV/c: mass ordering
- $p_T \sim 2.5$ GeV/c: crossing between v_2 of baryons and mesons
- $p_T > 2.5$ GeV/c: baryons $v_2 >$ mesons v_2 (flow driven by quark content)
- Light nuclei participating in flow

(Anti)deuteron v_2 and v_3 in Pb-Pb

Phys. Rev. C 102 (2020) 055203



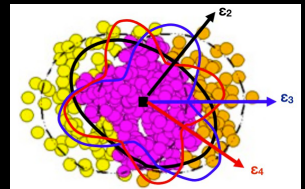
- Coalescence model with phase-space distributions of protons and neutrons from iEBE-VISHNU in agreement with data

Correlations between flow amplitudes

Observables sensitive to initial state and dynamical evolution of QGP

Symmetric cumulants

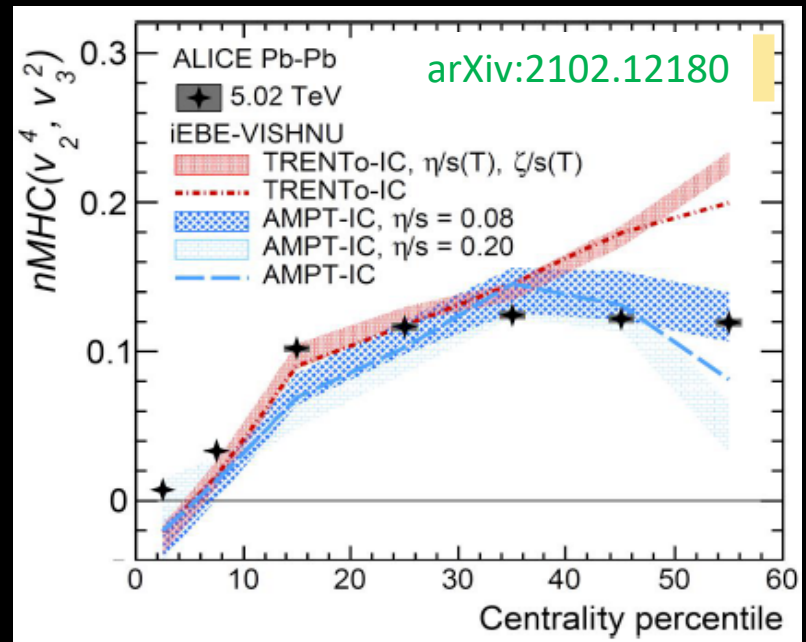
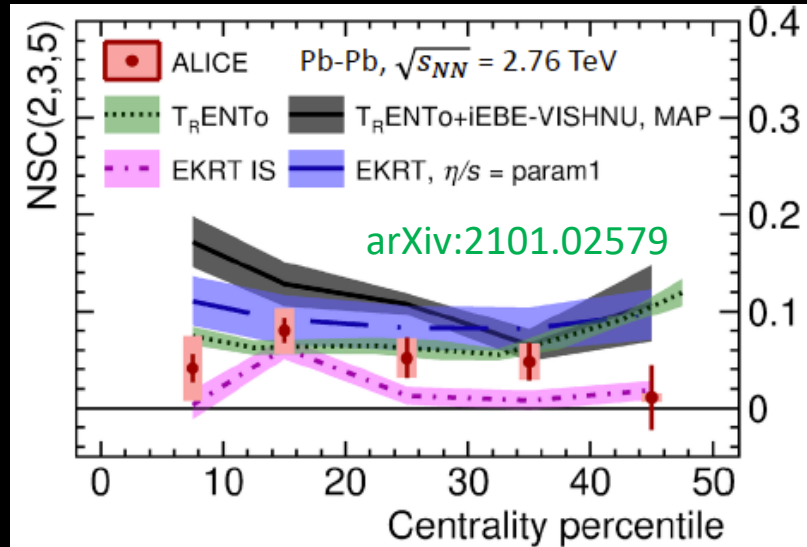
$$SC(k, l, m) \equiv \langle v_k^2 v_l^2 v_m^2 \rangle - \langle v_k^2 v_l^2 \rangle \langle v_m^2 \rangle - \langle v_k^2 v_m^2 \rangle \langle v_l^2 \rangle - \langle v_l^2 v_m^2 \rangle \langle v_k^2 \rangle + 2 \langle v_k^2 \rangle \langle v_l^2 \rangle \langle v_m^2 \rangle$$



$$NSC(k, l, m) \equiv \frac{SC(k, l, m)}{\langle v_k^2 \rangle \langle v_l^2 \rangle \langle v_m^2 \rangle}$$

Mixed harmonic cumulants

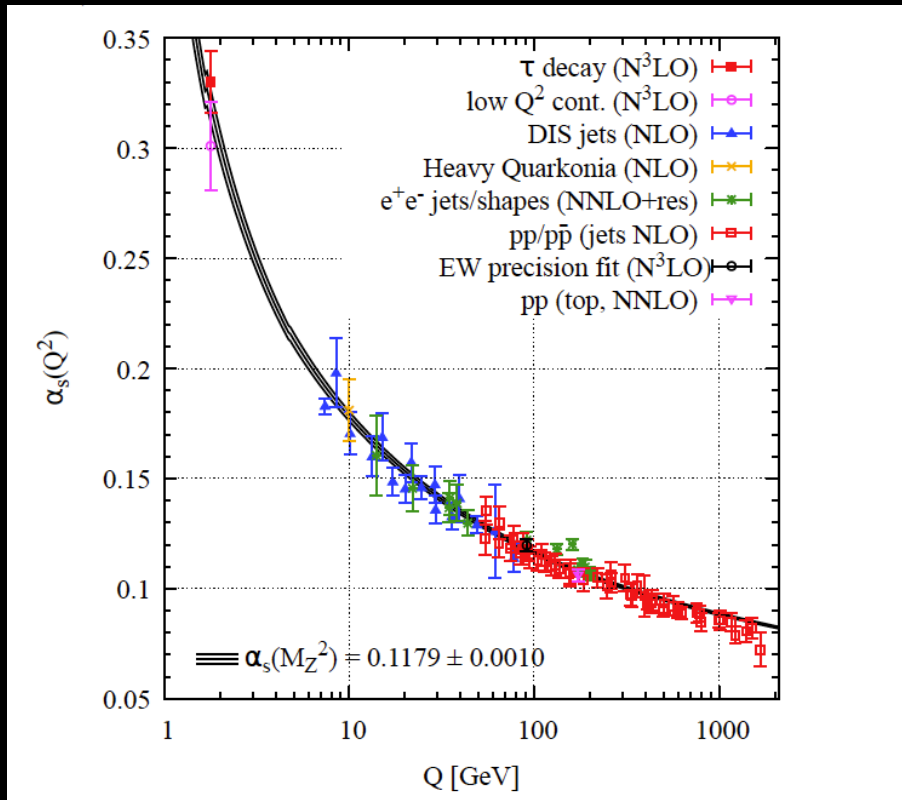
$$MHC(v_2^4, v_3^2) = \langle v_2^4 v_3^2 \rangle - 4 \langle v_2^2 v_3^2 \rangle \langle v_2^2 \rangle - \langle v_2^4 \rangle \langle v_3^2 \rangle + 4 \langle v_2^2 \rangle^2 \langle v_3^2 \rangle$$



- Symmetric cumulants and mixed harmonic cumulants are insensitive to non-flow contributions

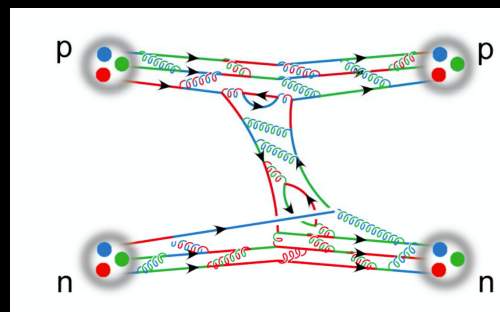
The strong interaction

PDG 2020



Running coupling constant α_s :

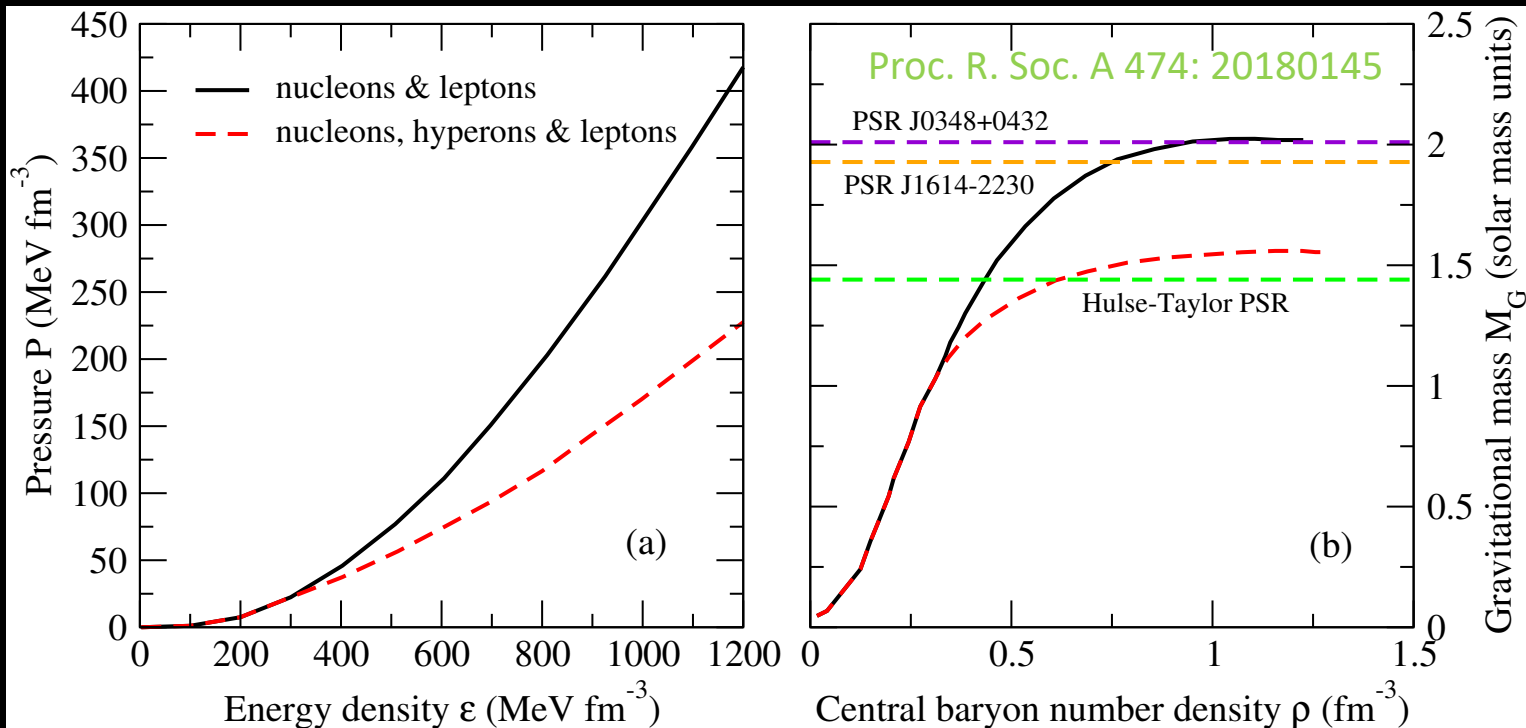
- Asymptotic freedom at small distance ($Q^2 \gg \Lambda_{\text{QCD}}^2$)
- Confinement at large distance ($Q \lesssim 1 \text{ GeV}$)
 - Perturbative methods not applicable
 - Effective theories with hadrons as degrees of freedom
 - Lattice QCD calculations



$$\alpha_s(Q^2) \equiv \frac{g_s^2(Q^2)}{4\pi} = \frac{12\pi}{(33 - 2N_f)\ln(Q^2/\Lambda_{\text{QCD}}^2)}$$

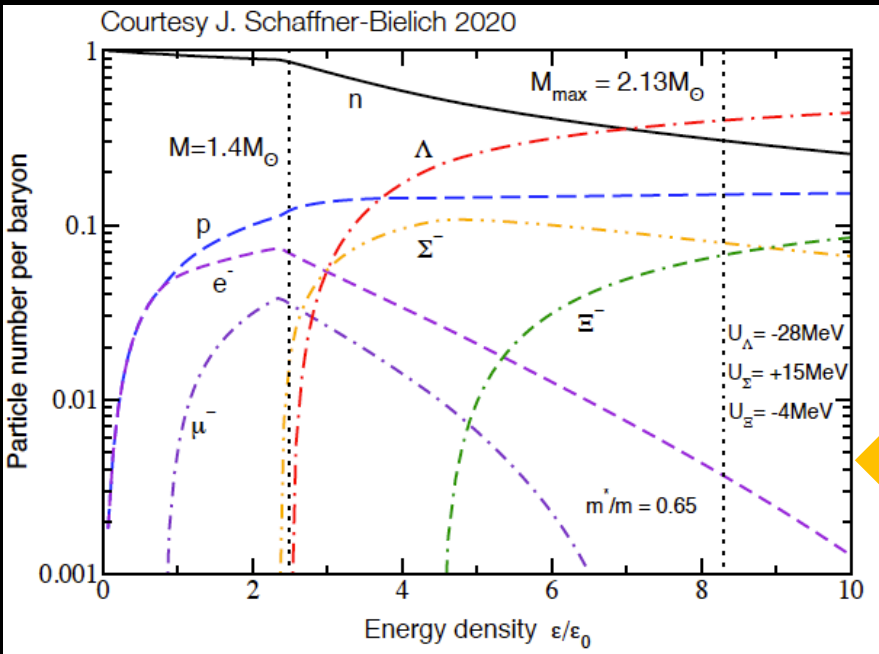
What is the strong interaction between different hadron species?

Hyperon puzzle

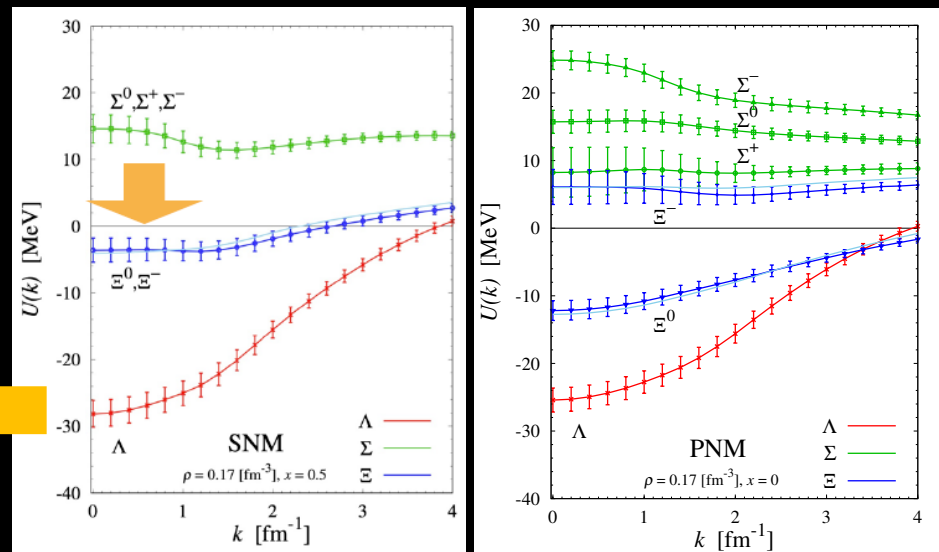


- Hyperons may appear in the inner core of neutron stars at densities of about $2-3\rho_0$
- Their presence in the neutron star interior leads to a softening of the EoS and consequently to a reduction of the maximum mass (current predictions $1.4-1.8 M_\odot$)
- Astrophysical observations of pulsars rule out almost all currently proposed EoS with hyperons...?
- Additional repulsion: Y-Y repulsive potential, hyperonic three-body forces (e.g. NNY, NYY, YYY), quark-gluon plasma below the hyperon threshold (hybrid neutron stars)...?

Hyperon puzzle and lattice QCD



HAL QCD, T. Ioune et al. AIP Conf. Proc. 2130 (2019) 1, 020002



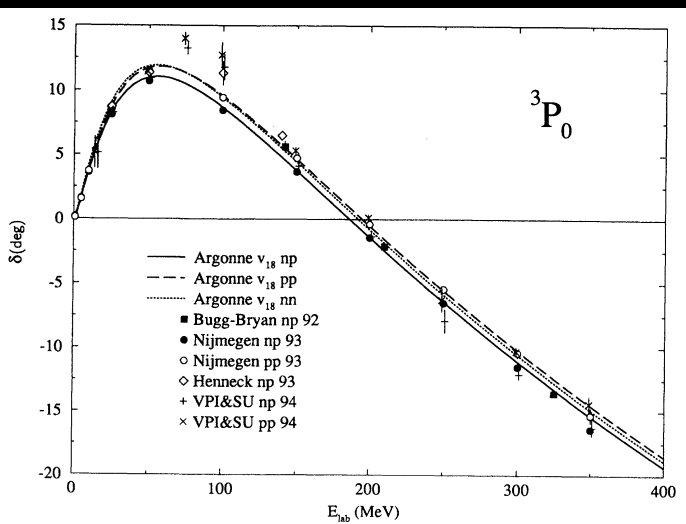
Hyperon single-particle potential

- Ξ^- attractive single-particle potential in symmetric nuclear matter (SNM) and repulsive in pure neutron matter (PNM)
- Ξ^- appears at larger densities in neutron stars

→ Resulting EoS of neutron stars is stiffer and matches astrophysical observation...

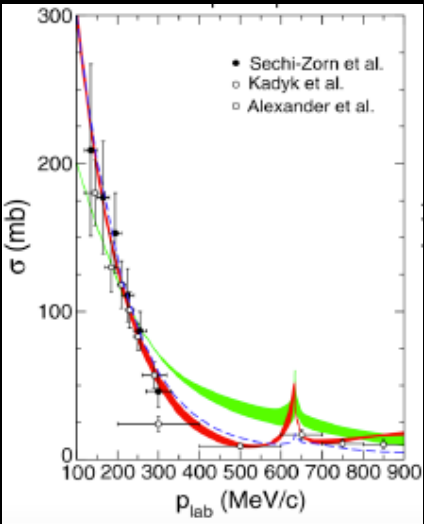
Experimental data to constrain the strong interaction

$N+N \rightarrow N+N$



R. B. Wiringa et al., PRC 51 (1995) 38

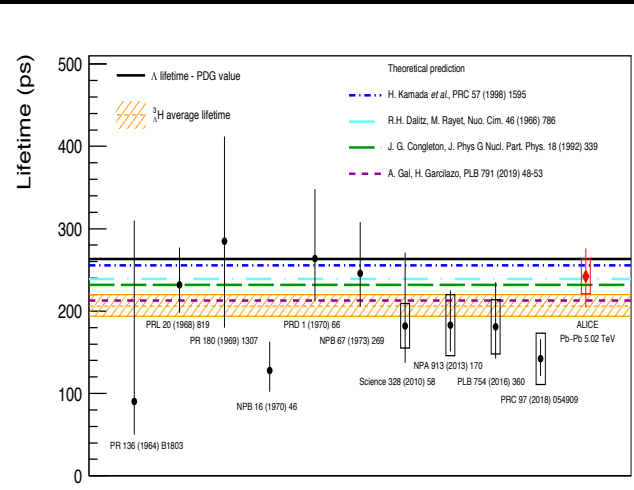
$N + \Lambda \rightarrow N + \Lambda$



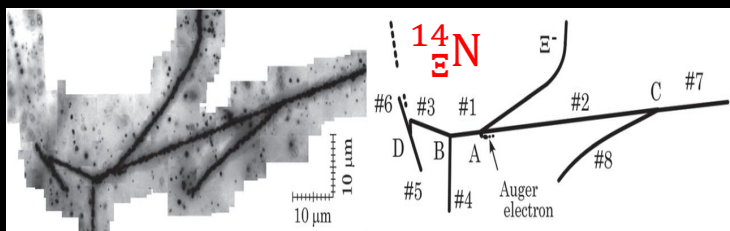
LO: H. Poinder et al. NPA 779 (2006) 244

NLO: J. Haindenbauer et al. NPA 915 (2013) 24

Hypertriton lifetime



ALICE PLB797 (2019) 134905

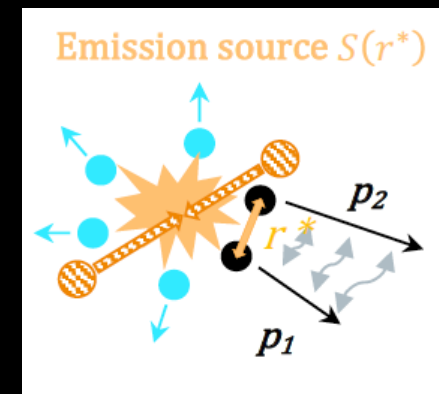
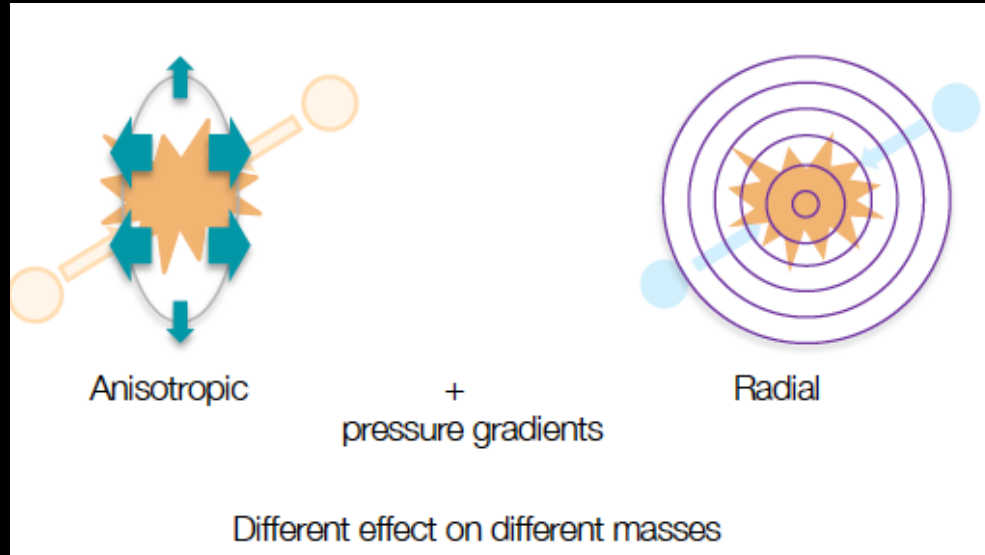


K. Nakazawa, PTEP 2015 (2015) 033D02

- Good constraints for NN interaction
- Small statistics of scattering data for hyperons
- ~1000 Λ -hypernuclei and one $^{14}_{\Xi}N$ discovered by now

Common baryon source

Collective flow and feed-down from short lived resonances modify source size



Resonances with $\text{ct} \sim r_0 \sim 1\text{fm}$ ($\Delta^{++}, N^*, \Sigma^*$)

Particle	Primordial fraction	Resonances $\langle \text{ct} \rangle$
Proton	33 %	1.6 fm
Lambda	34 %	4.7 fm

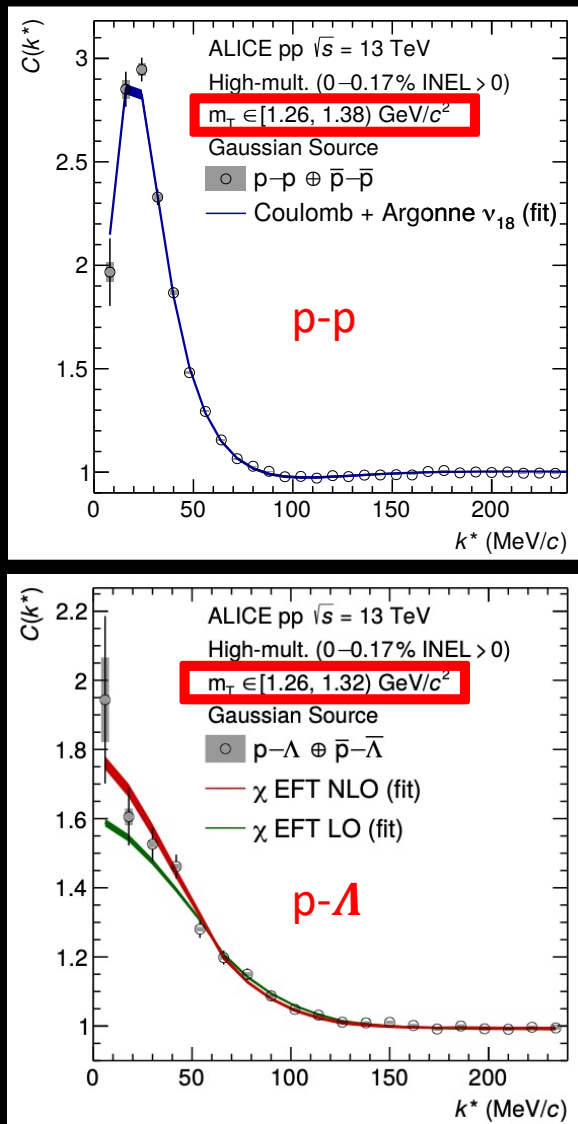
U. Wiedemann U. Heinz (PRC56 R610, 1997)

$$m_T = \sqrt{k_T^2 + m^2}, k_T = \frac{1}{2}|p_{T1} + p_{T2}|$$

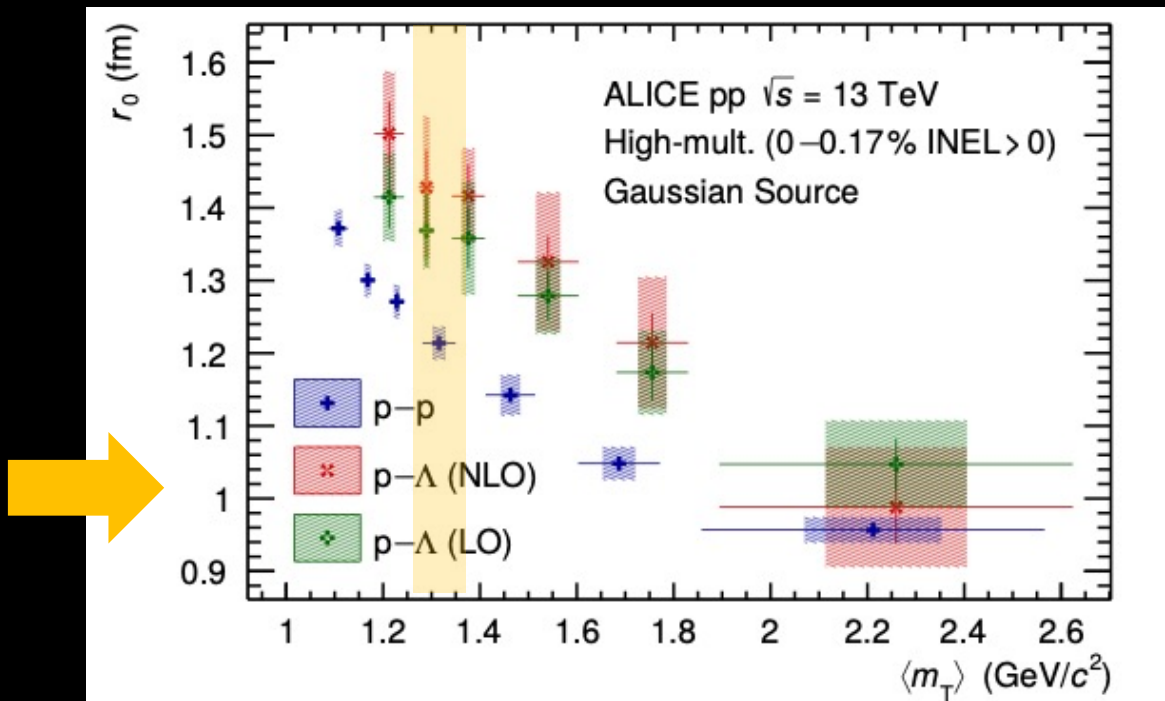
$$S(r^*) = G(r^*, r_{core}(m_T)) = \frac{1}{(4\pi r_{core}^2)^{3/2}} \exp\left(-\frac{r^{*2}}{4r_{core}^2}\right) \otimes E(r^*, M_{res}, \tau_{res}, p_{res})$$

$$E(r^*, M_{res}, \tau_{res}, p_{res}) = \frac{1}{s} \exp\left(-\frac{1}{s}\right), S = \beta \gamma \tau_{res} = \frac{p_{res}}{M_{res}} \tau_{res}$$

Common baryon source



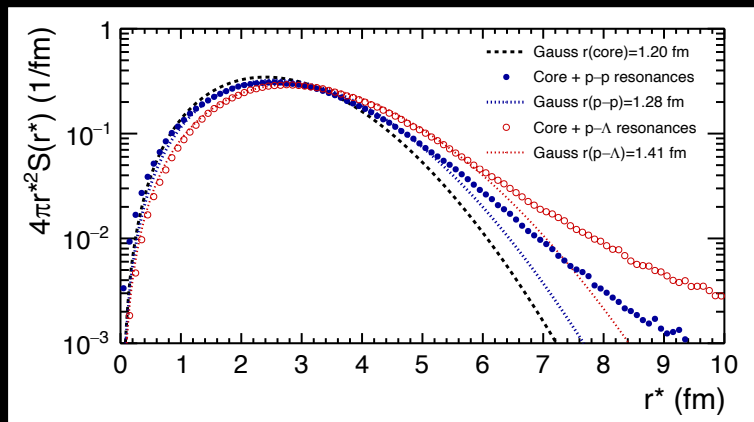
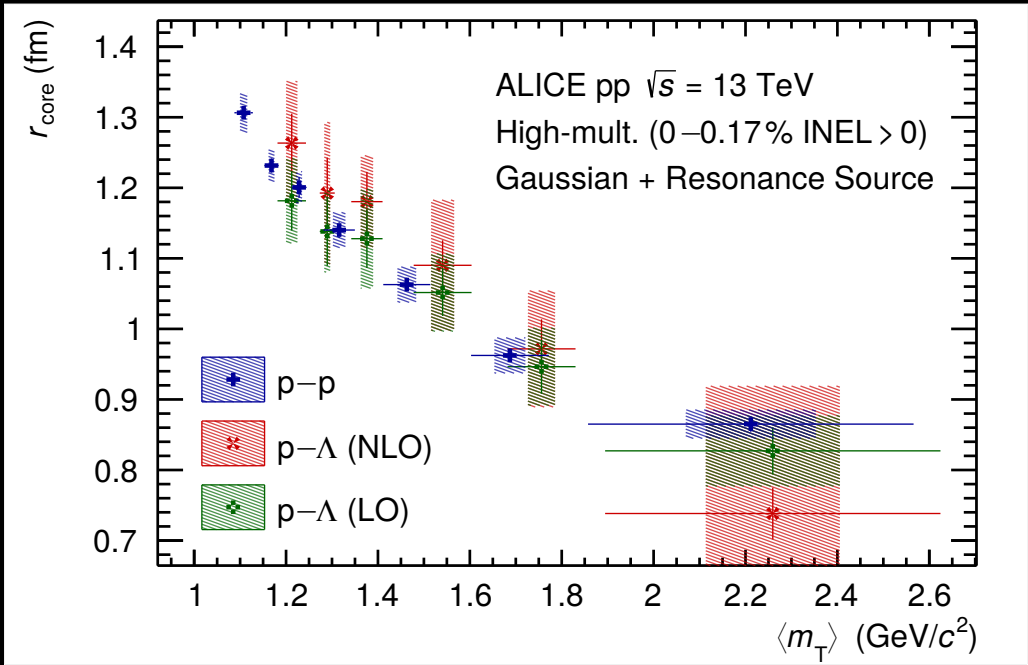
ALICE PLB 811 (2020) 135849



- Different source size depending on the baryon pair
- Gaussian source scales with m_T

Common baryon source

ALICE PLB 811 (2020) 135849



- Relative particle abundances from Statistical Hadronization Model *
- Kinematic distributions from EPOS **

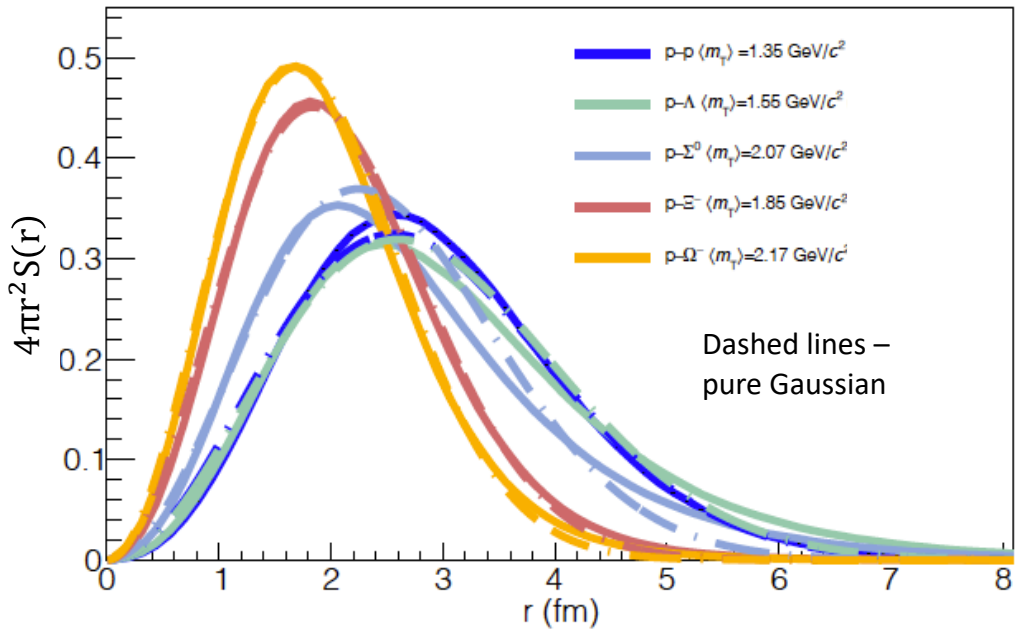
- All baryon pairs with included resonances show common m_T scaling
 → Indication of common baryon source
 → One can use p-p correlation to fix source size for other baryon pairs

* F. Becattini et al. J. Phys. G: Nucl. Part. Phys. **38** 025002

** T. Pierog et al. PRC 92 (2015) 034906

Common baryon source

Source using a Gaussian core plus resonances



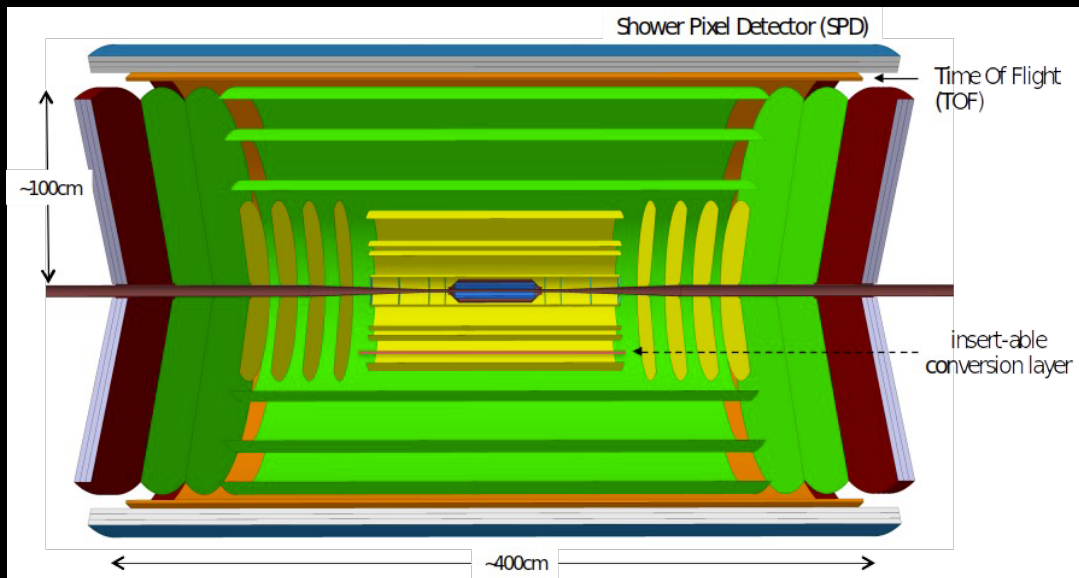
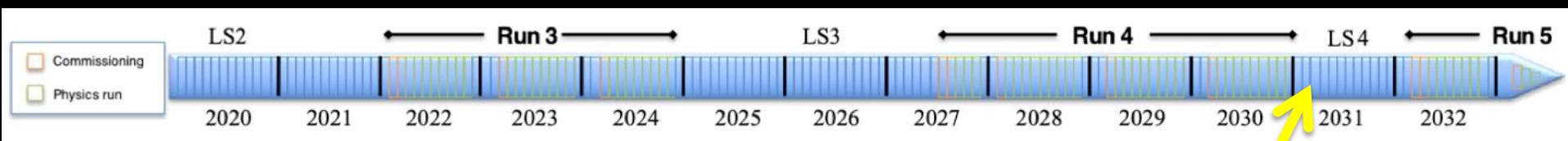
Pair	r_{Core} [fm]	r_{Eff} [fm]
p-p	1.1	1.2
p-Λ	1.0	1.3
p-Σ⁰	0.87	1.02
p-Ξ⁻	0.93	1.02
p-Ω⁻	0.86	0.95

- Emission source for heavier pairs using p-p correlation function plus resonances
- Gaussian source with $r_{\text{eff}} = 1.02 \pm 0.05$ (0.95 ± 0.06) fm used for the p-Ξ (p-Ω) emission

Future Heavy Ion Detector

Possibility to extend heavy ion measurements at the LHC beyond 2030

arXiv:1902.01211



Physics:

- Heavy flavor and quarkonia
- Low mass dielectrons
- Soft photons and hadrons
- BSM

Design guidelines:

- All silicon detector
- High rate capability: $\sim 10^{34}/\text{cm}^2/\text{s}$ ($\sim 50x$ Run3-4)
- Vertex spatial resolution: $\sim 1 \mu\text{m}$
- Tracking over wide kinematic range
 - $30 \text{ MeV}/c < p_T < 10 \text{ GeV}/c$
 - $|\eta| < 4.0$